2014

Temporal Variability of Particulate Organic Carbon Fluxes in the Northern Gulf of Mexico

Somiddho Bosu
Louisiana State University and Agricultural and Mechanical College

TEMPORAL VARIABILITY OF PARTICULATE ORGANIC CARBON FLUXES IN THE NORTHERN GULF OF MEXICO

A Thesis

Submitted to the Graduate Faculty of the
Louisiana State University and
Agriculture and Mechanical College
in partial fulfillment of the
requirements for the degree of
Master of Science

in

The Department of Oceanography and Coastal Sciences

by
Somiddho Bosu
B. Sc., Presidency College, Kolkata, 2009
M. Sc., Indian Institute of Technology, 2011
August 2014

Acknowledgement

I would like to take this opportunity to thank my advisor, Dr. Kanchan Maiti, for all his support, guidance and advice during last 2 years. I also owe a great deal of gratitude to my committee members Dr. Sibel Bargu Ates and Dr. Sam Bentley. They provided valuable guidance and useful comments throughout this experience. I would like to thank all my committee members for the time and effort they have given to my thesis. This study would not have been possible without the help and support from my lab mates. I would like to thank Puspa Adhikari for his camaraderie during the cruises. Patrick Jones also helped with sample collection and provided valuable technical support. I also want to thank Mr. Charles Milan for assistance with CHN analysis. Also, I would like to thank Dr. Eurico D'Sa and Dr. Malinda Sutor, for their assistance in providing the ancillary satellite and biological productivity data used in this study. This study would not have been possible without the help from the captain and crew of the R/V Walton Smith.

Finally, I would like to thank my parents, for all their support and encouragement during my graduate studies. I could not have done this without them. Also, I am extremely grateful to my friends David Reeves, Ryan Munley, Jie Li and others for the encouragement I received from them. This project was funded by the Louisiana Board of Regents.

Table of Contents

Abstract

There is limited data of Particulate Organic Carbon (POC) export from the Northern Gulf of Mexico and this work presents the first estimation of the efficiency of the "biological pump" in this region. In oligotrophic oceans like the Gulf of Mexico, POC is the main source of particles and POC flux is the key mechanism for the removal of particle reactive contaminants and pollutants from upper ocean water column. Particle-reactive, the naturally occurring radionuclides are useful tracers of the sinking flux of organic matter from the surface to the deep ocean. The disequilibrium between natural radioisotope pair ^{238}U-^{234}Th as well as sediment traps have been widely used to measure particle export fluxes from surface ocean water column. Another radionuclide pair, ^{210}Pb-^{210}Po, can also be used for the same purpose but has not been as widely adopted till now. The present work measured the vertical profiles of total and particle size-fractionated ^{210}Po and ^{234}Th activities, together with Particulate Organic Carbon (POC) concentrations during an opportunistic cruise in the month of April in 2012 and 2013 in and around the Deep Water Horizon spill site (28°44'N, 82°22'W) in the Gulf of Mexico. Both ^{210}Po and ^{234}Th reasonably predict sinking POC fluxes, caught in sediment traps, and each tracer provides unique information about the magnitude and efficiency of the ocean's biological pump. POC flux estimates ranged between 22-41 $mgCm^{-2}day^{-1}$ at 150m to 9-29 $mgCm^{-2}day^{-1}$ at 350m. POC export efficiencies ranged between 0.54-4.25% at 150m to 0.43-3.08% at 350m and showed an inverse linear relation with the surface productivity, contrary to the idea that higher primary productivity leads to higher export. However more research is needed to better understand the biological pump in this context, which not only impacts the atmospheric CO_2 sequestration, but also is the main source of nutrient to benthic organisms.

Chapter 1. Introduction

1.1 Background and Motivation

The "biological pump", active in the upper ocean water column, plays an important role in natural carbon sequestration. Autotrophic organisms in the photic zone capture CO_2 from atmosphere during photosynthesis, to form organic material, which is transferred throughout the food web in the upper ocean. A portion of this carbon is transported through the water column as Particulate Organic Carbon (POC). POC is partly remineralized due to microbial and grazing activity and the rest of the POC continues through the water column and reaches the benthic zone. POC is the main source of nutrients for benthic organisms (Honjo et al., 2008; Rocha and Passow, 2007) and the unutilized carbon is deposited with sediment. This complete process (atmospheric CO_2→photosynthesis→POC flux→deposition) is referred to as the "biological pump", and is one of the major natural CO_2-sequestration processes. Global estimates from radiometer data shows annual sea surface production to be 45–50 Giga-ton of Carbon (Longhurst et al., 1995) while the predicted (algorithm from satellite data) amount of POC reaching the seafloor is 1.4-3.2 Giga-ton of organic carbon every year (Dunne et al., 2007). Along with surface production, a number of other factors also control POC flux, viz., morbidity of biomass, microbial recycling, zooplankton grazing and physical factors (Maiti et al., 2013). This implies that POC flux calculation from primary production data at the sea surface (either in situ or satellite based) can lead to erroneous estimation due to variability in these controlling factors. The ratio of surface-production/POC flux is the estimate of the export efficiency of the biological pump (Buesseler and Lampitt, 2008).

Direct measurement of POC flux is possible with sediment traps (Buesseler et al., 2000, 2007, 2013). Likewise, indirect estimation of POC flux is obtained from natural radio-isotope tracers- ^{238}U-^{234}Th (Buesseler et al., 1992) and ^{210}Pb-^{210}Po (Shannon et al., 1970; Bacon et al., 1976). Scavenging of ^{234}Th and ^{210}Po by the sinking particles disrupts the parent-daughter secular equilibrium of the isotope pairs and results in the difference of their activity (concentration) in upper ocean water column. The deficiency of the daughter isotopes quantifies particle flux. Depending on the half-lives of the daughter-isotopes, they represent flux averaged over different time periods. ^{238}U-^{234}Th represents a monthly flux rate ($t_{1/2}$=24 days), while ^{210}Pb-^{210}Po gives a seasonal flux rate ($t_{1/2}$=128 days) (Stewart et al., 2011).

POC flux estimates from the Gulf of Mexico are not extensive. Previous studies include POC flux estimated from sea surface production, derived from satellite data of phytoplankton pigment concentration (Biggs et al., 2008). This estimate of POC flux to seabed shows a spatial variability across the Gulf and ranges between ~9-18 $mgCm^{-2}day^{-1}$. Another study from this region used sediment traps and ^{238}U-^{234}Th disequilibrium method to estimate POC flux between upper 140m of water column. Their flux estimation ranges between 24-150 $mgCm^{-2}day^{-1}$ at 120m (Hung et al., 2010).

1.2 Research Objective

This study focuses on estimating POC flux below the euphotic zone of the Northern Gulf of Mexico (150-350m), utilizing 3 different methods, to estimate the export efficiency of the "biological pump". The variability and limited nature in the available data from this region clearly leaves a huge scope for research. Productivity in the surface ocean was measured from incubation experiments during the cruises, which was used to estimate export efficiency (see chapter 6). At the same time, utilizing three different methods of POC flux estimation helps look into its seasonal variability (see chapter 6).

In "oligotrophic" (low particle abundance) oceans like the Gulf of Mexico (Baskaran et al., 1992), where terrestrial particle source is insignificant, the major sinking particle pool is formed by biological activities in the upper ocean. Hence, understanding the organic particulate flux in the Gulf of Mexico will also help in understanding the removal mechanism of Polycyclic Aromatic Hydrocarbons (PAHs) and other similar particle reactive pollutants (Santschi et al., 2001). However, detailed study of PAHs removal mechanism was outside the scope of this study.

1.3 Field Area

Samples were collected during two opportunistic cruises in the Gulf of Mexico during the month of April in 2012 and 2013, on board R/V Walton Smith. Sampling was done in 3 stations— North of Deep Water Horizon (NDWH), on Deep Water Horizon (DWH) and South of Deep water Horizon (SDWH). Each year sediment traps were deployed in DWH and SDWH. Niskin samples were collected for both ^{238}U-^{234}Th and ^{210}Pb-^{210}Po analysis, from all three stations. Large volume submersible pumps were deployed to collect size fractionated particulate samples for POC, ^{234}Th and ^{210}Po analysis as well (see Figure 1.1). From here onwards, the

sampling stations are referred to as NDWH 12, DWH 12, SDWH 12 for 2012 samples, and NDWH 13, DWH 13. SDWH 13 for 2013 samples.

The location of the stations were so chosen, that it was away from any coastal influence, in the open ocean (~50miles, 80km from nearest coast). Satellite derived Sea Surface Chlorophyll (SSC) data (Biggs et al., 2008) shows that this region experiences a seasonal change of productivity (Figure 1.2).

Station	SDWH 12/13						DWH 12/13						NDWH 12/13					
Deployment	Water	Pump-1	Trap-in	Water	Pump-2	Trap out	Water	Pump-3	Trap-in	Water	Pump-4	Trap out	Water	Pump-5	~~Trap-in~~	Water	Pump-6	~~Trap-out~~
Depth [m]	10 100 150 250 350 750		150 250 350	10 750	100 150 250 350	150 250 350	10 100 150 250 350 750		150 250 350	10 750	100 150 250 350	150 250 350	10 100 150 250 350 750			10 750	100 150 250 350	

Figure 1.1. Schematic of deployments and sample collection in 2012 and 2013 cruises.

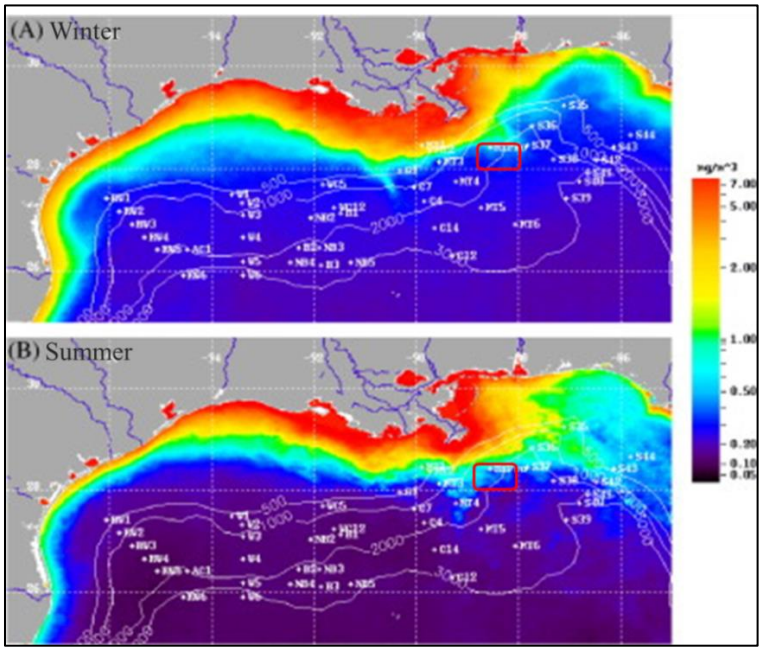

Figure 1.2. Sea Surface Chlorophyll image after Biggs et al., 2008. Red square shows sampling location of this study. Seasonal change of SSC concentration inside the boxes is evident.

This indicates possibility of a seasonal change of POC flux in this area as well. The change of POC flux is expected to be documented in the different methods of flux estimation. Sediment trap and ^{234}Th derived flux will represent the lower productivity period of summer, while the same from ^{210}Pb-^{210}Po will represent the Spring-bloom period (see discussion in chapter 5).

The on-board CTD-profiler of R/V Walton Smith was used to collect salinity, oxygen, florescence-chlorophyll and temperature profiles of the sampling locations (Figure 1.3). General trend of salinity was straight-vertical in upper waters with an observable decrease with depth.

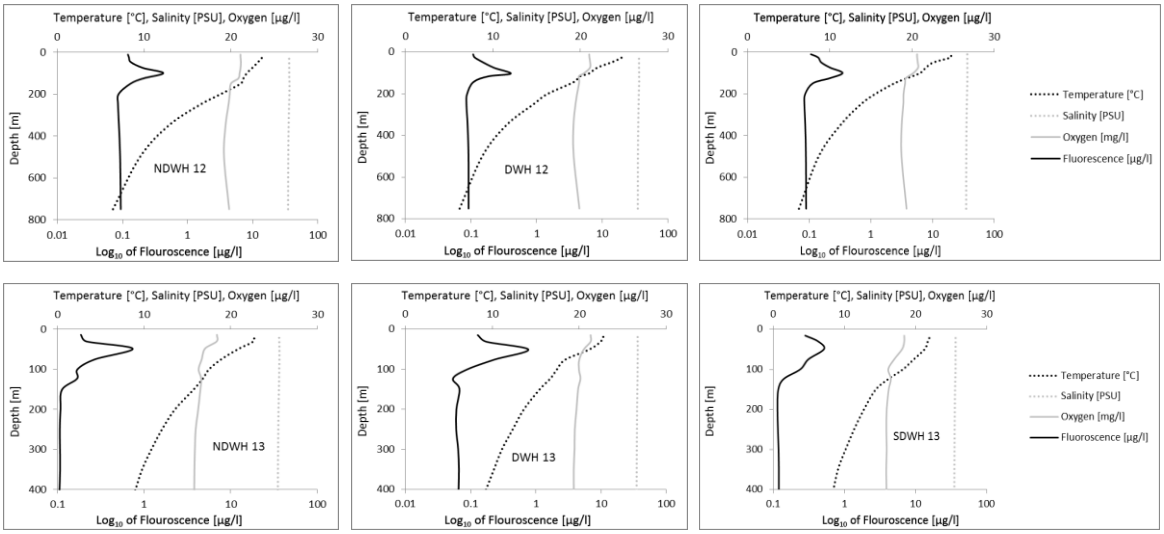

Figure 1.3 Salinity, temperature, oxygen and fluorescence profiles from SDWH in 2012 and 2013. Acquired with the CTD profiler of R/V Walton Smith.

The mixed layer was identified by vertical temperature curve up to 30-50m. Below the mixed layer, temperature decreased steadily with depth. At all stations, chlorophyll-fluorescence peaks were observed at the base of the mixed layer (40-70m). Dissolved oxygen is elevated within the surface mixed layer. Bellow the mixed layer, the peak conforms to the chlorophyll maxima and follows the overall trend of chlorophyll profile thereafter. The oxygen minima layer is observed between 200-400 m and is correlated with the influence of the Gulf Loop Current (Morrison and Nowlin, 1977).

Sea Surface Height (SSH) and Sea Surface Temperature (SST) satellite-data from the region in 2012 shows presence of a warm core eddy waters occupying the area North of DWH while the colder waters occupied the stations South of DWH (Figure 1.4). The Loop Current is

conspicuous from 2013 SSH and SST data. The current extends up to ~25°N, which is outside the sampling location. A remnant eddy is visible at South of DWH in 2013. Over the DWH site, a cyclonic cold core eddy is visible which entraps a cooler plume from the shelf waters on its northwestern edge in 2013 (see Figure 1.4).

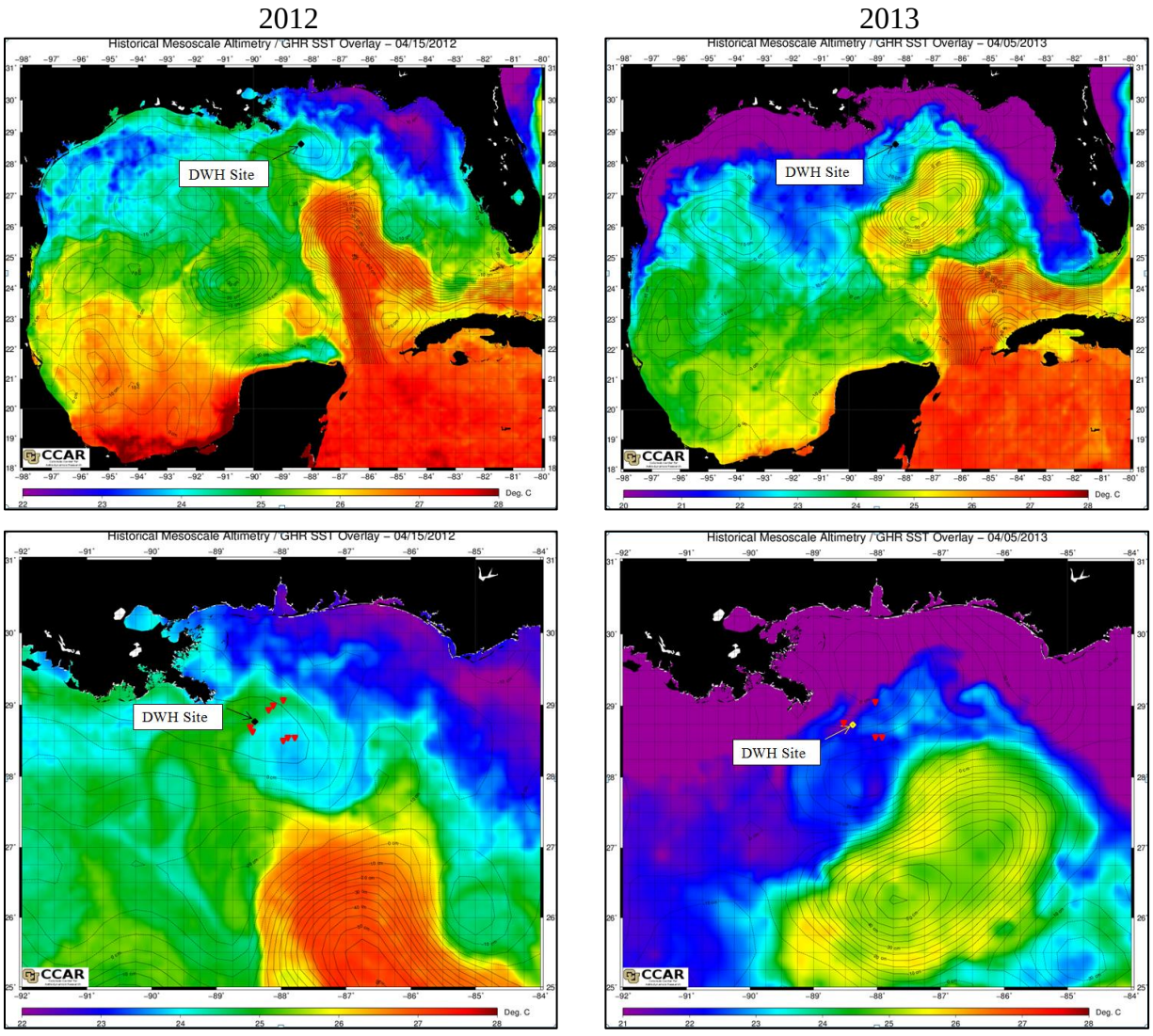

Figure 1.4. Sea Surface Height (SSH) anomaly contours overlaid on Sea Surface Temperature (SST) image of the Gulf of Mexico. April 15 in 2012 and 2013.
(http://eddy.colorado.edu/ccar/ssh/hist_gom_grid_viewer)

Chapter 2. Sediment Traps Derived POC Flux

2.1 Introduction

Sediment traps have traditionally been used to estimate particle flux in the ocean from the 1970s (Honjo, 1976). The merit of sediment trap derived flux lies in its direct principle, which is similar to rain gauges (Buesseler et al., 2000). However there are several sampling biases and the trap derived fluxes are found to be inconsistent in available literature (Buesseler et al., 2007; Buesseler, 1991). The major identified biases in trap sampling are caused by hydrodynamics, swimmer (zooplankton) infiltration and solubilization of particles inside the trap (Buesseler et al., 2007). Surface ocean (0-1000 m) typically has profound current influence. Strong currents close to the trap opening can re-suspend already settled particles. Current can also tilt the trap from its preferred vertical position, influencing the particle influx (Gardner, 1985). Under the strong currents of upper ocean, surface tethered drifting sediments traps (Particle Interceptive Traps- PITs) are found to be more effective in minimizing hydrodynamic effects. In contrast to its bottom moored counterpart, PITs can drift along the flow, which minimizes its interference with current (Buesseler et al., 2007). Simultaneously, plastic baffles are used at the trap opening, to minimize resuspension of particles from inside the trap cylinder. These baffles also help in keeping out the zooplanktons which are lured by the abundant food available inside the traps and swim in. Shape of sediment traps has also been optimized over time. Cylindrical traps are found to be more dependable in flux estimation (Butman, 1986) and are designed following a specific aspect ratio (Lamborg et al., 2008). Remineralization of particles inside the trap is another potential source of underestimation of flux. Preservative is added to the traps, and traps are recovered within a reasonable time to prevent extensive remineralization (Lee et al., 1992).

The lack of any standardized design and the continuous effort to improve the same also causes inconsistency in sediment trap data found in literature. For example, Pace et al. (1987) showed in NE-Pacific, that particle flux is directly proportional to surface production using sediment trap data. This direct relation was widely used as a benchmark to cross check trap derived flux, until recent studies came up with an inverse relationship between production and export (Maiti et al., 2013). In order to perfect the design and to understand the processes influencing sediment trap flux, a number of experimental studies have been done in laboratories (Gardner, 1980; Butman et al., 1986; Hawley, 1988). Also, attempts were made to "calibrate" trap derived flux with other methods of flux estimation (Buesseler, 1991). Recently, Neutrally

Buoyant Sediment Traps (NBST) have been introduced and are found to be more effective in optimizing flux estimates compared to surface tethered traps (Buesseler et al., 2000). However NBSTs are still under the process of development. In contrast, PITs are standardized, and are used extensively in upper ocean flux estimation, e.g., in Joint Global Ocean Flux Study (JGOFS), Bermuda Atlantic Time Series (BATS), Hawaii Ocean Time Series (HOTS) and numerous other studies.

2.2 Trap Deployment and Recovery

In this study, surface tethered drifting Particle Interceptive Traps (PITs) were used to collect settling particulate samples. The design of the trap array was similar to PITs systems used in JGOFS, HOTS and BATS with slight modification (Lamborg et al., 2008). Traps were deployed for 2.5-3.0 days at each station. A surface buoy was used to keep the array afloat. In order to dampen the surface wave action on the trap array, a second buoy was deployed at 50m depth, hooked to the surface-buoy with a bungee. Below the second buoy, the rest of the trap array was attached with synthetic links, long enough to deploy traps at target depths. The array had one set of traps at 3 different depths (150m, 250m and 350m). Cylindrical traps were attached to 3 X-frames at these depths. Individual sets of traps had 8 cylindrical traps (diameter=12cm, height=60cm; H/D ratio=5) to collect replicate samples from each depth. Before deployment, the trap-cylinders were filled with filtered (1 μm Melt Blown Filter Cartridges) seawater collected from the depth of deployment. After that, 500ml poisoned brine solution was directly injected to the bottom of the cylinders, below the sea water. 0.02% formaldehyde was added as poison to the brine (lee et al., 1992). Borate was used as buffer, to stabilize the formaldehyde. Formaldehyde solution retards bacterial activities and prevents solubilization of organic matter, collected at the bottom of the trap cylinders (Owens et al., 2013). A plastic honeycomb baffle was fitted near the trap opening.

A strobe, a radar reflector, a VLF transmitter and an Argos GPS locator were fixed to the surface-buoy to find its location during recovery. The position of the trap array was continuously monitored during the period of deployment and the ship maintained a maximum distance of 10 miles from the array. After the scheduled deployment time was over, the trap was located using the instrumentation mentioned above and was retrieved using the on board crane of R/V Walton Smith.

Several hindrances were met during the sediment trap deployments in this study. In the 2012 cruise, traps could not be deployed in NDWH as planned, due to inclement weather. In 2013, during the second deployment, the deepest set of trap was cut off from its link and lost (probably tangled and tore off thereafter by the tag line of a seismic boat). During recovery, the GPS tracker pack on the buoy was hit by the steel hook of the on-board crane. The massive blow broke the casing and released the trackers into the sea. Due to the loss of GPS and other trackers, the 3rd deployment (NDWH) was cancelled in 2013 too. As a result, we have sediment trap derived flux from only two stations (DWH and SDWH) from both the years.

2.3 Analyses of Sediment Trap Flux

The traps were left to stand for at least 1 hour after recovery, to allow time for the in-tube particles to settle into the bottom brine layer. The seawater inside the traps was siphoned out to just above the visible density boundary on top of the brine layer. Then the brine was taken out through the tap at the bottom of the traps, and passed through acid-washed nylon mesh (1 µm pore) in Teflon filter holder (Savillex) to remove swimmers. The filtered solution was again filtered through 25mm diameter 1µm QMA filters. The filters were dried at 60°C and preserved. For POC, ^{234}Th and ^{210}Po flux estimation, 3 replicate filter samples were used from each depth. ^{234}Th and ^{210}Po contents were also analyzed in settling particles to compare with results of flux estimated from water samples (see Chapters 3 and 4). Four of the trap samples were used for particulate Polycyclic Aromatic Hydrocarbons (PAHs) analysis and one was used for DNA analysis.

One replicate filter from the trap samples was exclusively used for POC analysis. Another duplicate POC analysis was done from the ^{234}Th sample filters after β counting in RISØ analyzer (developed by the Center for Nuclear Technologies, Technical University of Denmark), because RISØ-analysis is non-destructive. 12mm punches were subsampled from the 25mm filters using stainless steel punch. The 12mm punches were exposed to concentrated HCl vapor for 24 hours to eliminate any inorganic carbon present in the samples (Stewart et al., 2011; Pike and Moran, 1997). After fumigation, filters were dried at 60°C. Sample blanks were prepared using the same materials and method. The samples and the blank filters were wrapped inside silver capsules. Atropine ($C_{17}H_{23}NO_3$) was used as standard (Costech Analytical Technologies, Inc.). The samples, blanks and standards were run in Perkin Elmer Series II CHNS/O 2400 analyzer. Blanks and standards were run after every 10 samples in order to monitor stability of the instrument during analysis.

2.4 POC Flux Calculation

POC fluxes in sediment traps can be calculated directly from the analyzed organic carbon, the area of the trap opening (113.14 cm^2) and the duration of deployment (2-3 days). The following equation was used to calculate POC flux –

$$Flux_{poc} = POC/(Area_{trap} * Time_{deployment}) \quad – [I]$$

Replicate analyses were used to obtain an average of the POC flux from same sediment trap. Error was estimated as the standard deviation of the replicates.

2.5 Results and Discussion

In this study sediment traps were deployed during the month of April in 2012 and 2013. POC flux at 150m was comparatively higher in 2012 (29.04-31.52 $mgCm^{-2}d^{-1}$) than 2013 (22.79-22.95 $mgCm^{-2}d^{-1}$). Zooplankton grazing and bacterial activity cause remineralization of POC in the water column and POC flux decreases with depth (see Figure 2.1). Remineralization in water column is quantified as the fraction of POC flux loss over a certain depth (Table 2.1). Remineralization between 150-350m was higher in 2012 (0.62-0.71), compared to 2013 (0.44). Due to the higher remineralization, despite of the higher POC flux at 150m in 2012, POC flux at 350m was lower in 2012 (9.24-10.97 $mgCm^{-2}d^{-1}$), in comparison to the same in 2013 (12.72 $mgCm^{-2}d^{-1}$). The slopes of POC flux trend lines are steeper in 2013 (11.11-17.09) compared to the slopes in 2012 (8.82-10.97). This implies that, in 2012 POC flux change over depth was more drastic compared to 2013. In 2012, remineralization was lower between 150-250m (0.27-0.26), increased with depth, and was higher between 250-350m (0.60-0.49). In contrast, 2013 had higher remineralization between 150-250m (0.37-0.39) and remineralization decreased between 250-350m (0.11). In both the years, total remineralization between 150-350m water column shows a linear relationship with the POC flux at 150m (see Figure 2.2).

Sediment trap derived POC flux data from our study was compared with the only other available sediment trap study from the Gulf of Mexico (Hung et al., 2010). Hung et al deployed sediment traps in August 2005 and May 2006. Their main aim was to look into particle dynamics up to 140m. Our study was more focused on the particle dynamics below the euphotic zone (150m-350m) to estimate remineralization and export efficiency (see discussion in Chapter 1 & 6) and the shallowest trap was deployed at 150m. POC flux estimated by Hung et al. (2010) at 140m in August was 70-116 $mgCm^{-2}d^{-1}$, while the same in May was 27-61 $mgCm^{-2}d^{-1}$.

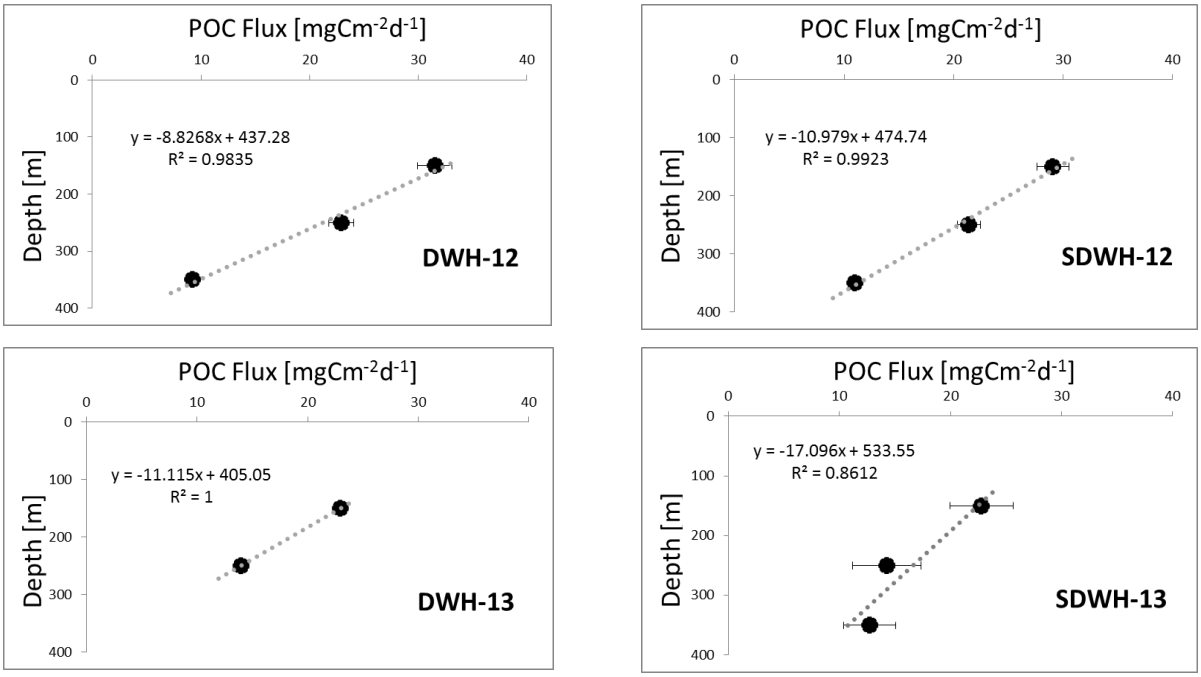

Figure 2.1. Trap derived POC flux from 2012 and 2013 cruises. POC flux shows a linear decrease with depth in all rpofiles (see Table 2.1).

Table 2.1. Trap derived POC flux from 2012 and 2013 cruises in $mgCm^{-2}d^{-1}$. POC flux decreases with depth (see Figure 2.1). Remineralization is high in stations with higher POC flux at 150m and low in stations with lower POC flux at 150m (see Figure 2.2).

Depth [m]	DWH 12	SDWH 12	DWH 13	SDWH 13
150	31.52 ±3.15	29.04 ±2.90	22.95 ±0.18	22.79 ±2.83
Remineralization%	27	26	39	37
250	22.88 ±2.29	21.39 ±2.14	13.95 ±0.24	14.25 ±3.07
Remineralization%	60	49	—	11
350	9.24 ±0.92	10.97 ±1.10	—	12.72 ±2.36
Σ Remineralization%	71	62	—	44

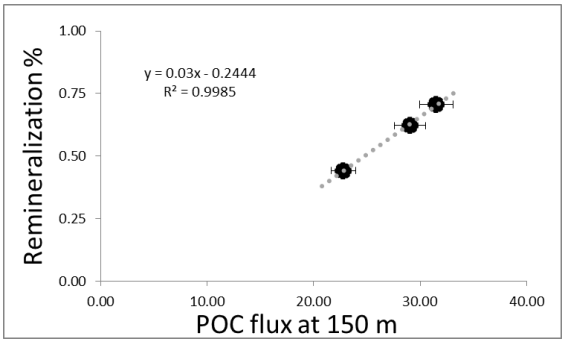

Figure 2.2. Plot of POC flux at 150m vs total remineralization between 150-350m. 150m POC flux shows a linear relationship (R^2= 0.99) with total re-mineralization at 350m.

Estimated POC flux from both the studies, at 140-150m in April-May is within range of error (22-32 and 27-61 $mgCm^{-2}d^{-1}$) and corroborates each other (see Table 2.2).

Due to the dearth of available sediment trap data from the Gulf of Mexico, a study from another oligotrophic ocean was chosen to compare our data. Bermuda Atlantic Time-series Study (BATS) site is an oligotrophic ocean with very low terrestrial influence, analogous to the Northern Gulf of Mexico. The study at BATS was done in November 2006 to March 2007 (Stewart et al., 2011). Sediment trap derived flux showed similar trend with depth and was slightly higher than our flux estimates (Table 2.2). One of the BATS stations had very low productivity (357.6 mg $Cm^{-2}d^{-1}$) and as a result remineralization was very low. The other two sites had remineralization comparable to our study (average 38% between 150-200m; 50% between 200-300m; and total 69% between 150-300m water column).

Table 2.2. Comparison of sediment trap derived POC flux from this study (GOM 12-13), Hung et al., 2010 (Gulf of Mexico), and Stewart et al., 2011 (BATS).

POC flux in $mgCm^{-2}d^{-1}$	GOM 12-13 April	Hung et al., 2010 May	Stewart et al., 2011 Nov-March
140-150	23-32	27-61	22-106
200-250	13-23	-	18-66
300-350	9-13	-	18-26

Chapter 3. Natural Radioisotope Tracers for POC Flux Estimation

Naturally occurring radioisotope tracers have been used for a long time to estimate particle fluxes in upper ocean. Radioisotope tracers were first suggested as a replacement of sediment trap derived flux estimation method, because the former is less expensive and less prone to failure (Buesseler, 1991). In this study, parent daughter isotope pairs ^{238}U-^{234}Th and ^{210}Pb-^{210}Po were applied to understand the POC fluxes in upper ocean. All four of these radioisotopes form a part of the natural ^{238}U decay series (Figure 3.1).

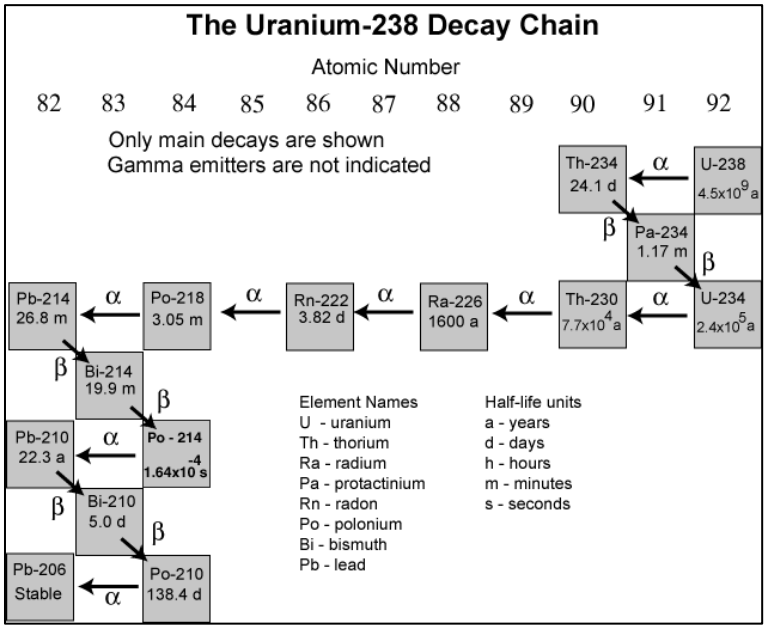

Figure 3.1 ^{238}U decay series. Diagram modified after http://pubs.usgs.gov/.

^{238}U is a conservative element in sea water, and vary as a function of salinity in global ocean. ^{234}Th is produced in ocean water by radioactive decay from its parent ^{238}U. Since both ^{238}U ($t_{1/2}$= 4.5 billion years) and ^{234}Th ($t_{1/2}$= 24.1 dyas) are radioactive elements and ^{238}U has a much longer half-life ($t_{1/2}$= 4.5 billion years) and compared to ^{234}Th ($t_{1/2}$= 24.1 dyas), in closed systems ^{234}Th activity should be in secular equilibrium with ^{238}U. Similarly, ^{210}Pb-^{210}Po should also remain in secular equilibrium in a closed system in absence of particles, due to the short half-life of ^{210}Po ($t_{1/2}$= 138.3 days) compared to its parent ^{210}Pb ($t_{1/2}$= 22.2 years). In open ocean ^{210}Pb is formed in-situ by decay of ^{226}Ra ($t_{1/2}$= 1600 years) (Broecker et al., 1967; Ku et al., 1970; Ku and Lin, 1976). However, excess ^{210}Pb can also be introduced in the system from atmospheric flux. ^{222}Rn is carried to the ocean from land sources and produces ^{210}Pb. ^{210}Pb

produced by decay of ^{222}Rn in atmosphere through multiple intermediate short-lived radionuclides, and is finally deposited to surface-ocean (Moore et al., 1974; Turekian et al., 1977; Kritz, 1983). On the other hand, ^{210}Po is produced in ocean water column only from in-situ decay of ^{210}Pb. ^{210}Pb decays to the intermediate short-lived radionuclide ^{210}Bi (5.01 days half-life), which in turn decays to ^{210}Po.

However, in upper ocean water column ^{238}U-^{234}Th and ^{210}Pb-^{210}Po isotope pairs are not in equilibrium, because the daughter isotopes of these pairs are particle reactive. As a result, ^{234}Th and ^{210}Po attach to sinking particles, and is scavenged from the upper ocean (Buesseler at al., 1992; Cochran, 1992). Due to scavenging with sinking particles, ^{234}Th and ^{210}Po are typically found to be depleted with respect to its parents in upper ocean. The extent of disequilibrium is used to quantify ^{234}Th and ^{210}Po fluxes (see discussion in chapter 4 and 5).

The activities of both parent and daughter isotopes are required from different depths in the water column to estimate loss of particle-reactive daughters with sinking particles from those depths. Since ^{238}U is a conservative element, its activity can be directly estimated from salinity of sea water (Chen et al., 1986). However of ^{234}Th, ^{210}Pb and ^{210}Po requires analysis of their total activities from sea water samples. For calculating flux, the activity differences of parent-daughter isotopes are calculated for different points in the water column and then integrated over depth between midpoints of two sampling depths (see discussions in Chapters 4 and 5). The following equation is used to estimate flux of daughter radioisotopes –

$$Flux_{Daughter} = \lambda \int (A_{Parent} - A_{Daughter})\, dz \qquad \text{-[3.1]}$$

Where, $Flux_{Daughter}$ is the flux of the daughter isotope, λ is the decay constant of the daughter isotope, A_{Parent} is the activity of the parent isotope in sea water and $A_{Daughter}$ is the activity of the daughter isotope at the same depth, and the difference of the parent-daughter activity is integrated over depth z, to estimate $Flux_{Daughter}$. The ratio of POC to daughter isotope in particles are used to convert $Flux_{Daughter}$ to POC flux (Equation 3.2).

$$Flux_{POC} = Flux_{Po} * (POC/ A_{Po})_{\ particulate} \qquad \text{-[3.2]}$$

Where $Flux_{POC}$ is POC flux, and $(POC/ A_{Daughter})_{\ particulate}$ is the ratio of daughter isotope to POC in particulate samples.

Chapter 4. ^{238}U-^{234}Th Derived POC Flux

4.1 Introduction

^{234}Th is produced in ocean water by radioactive decay of ^{238}U. Since both ^{238}U and ^{234}Th are radioactive elements, ^{234}Th activity in seawater should be in secular equilibrium with ^{238}U. However, ^{234}Th is particle reactive, while ^{238}U is a conservative element in sea water. As a result, scavenging of ^{234}Th by sinking particles in upper ocean causes its depletion with respect to ^{238}U (Buesseler at al., 1992). ^{238}U-^{234}Th disequilibrium in upper ocean water column was first reported by Bhat et al. (1969). The sampling behind this discovery was rather unplanned, suggested during a cruise on R/V Oceanographer, by Professor Rama of Tata Institute of Fundamental Research (TIFR, India). Samples were collected from the central Arabian Sea and analyzed in TIFR facility (Benitez-Nelson and Moore, 2006). The discovery of ^{238}U-^{234}Th disequilibrium opened a new possibility in quantifying particle flux in upper ocean. A relationship between surface productivity and ^{234}Th depletion in upper ocean was reported from the Pacific ocean (Coale and Bruland, 1985), and attempts were made to quantify particle flux from the residence time of particulate ^{234}Th (Eppley, 1989). However viability of this approach was questioned, as the residence time of particulate thorium and organic particulate matters are different in upper ocean (Murray et al., 1989). Interest in POC flux estimation from ^{238}U-^{234}Th disequilibria was renewed in early 1990s. ^{234}Th derived flux was suggested as a better tool than sediment traps in upper ocean (Buesseler, 1991) and a direct approach was developed, where ^{234}Th-flux is multiplied with POC/^{234}Th ratio to calculate POC flux (Buessler et al., 1992).

The major advantage of sediment trap derived flux over any proxy based flux estimation is that, a direct estimation can be obtained from sediment traps. However the sediment trap method comes with many drawbacks. The sampling biases as described in chapter 2.1 can be overcome by increasing the number of deployments, to obtain a statistically viable number of observations. That is not always feasible, because trap data come at an expense of long shiptime. Even if the shiptime could be afforded, in a high traffic sea like the Gulf of Mexico, it is very difficult to successfully deploy and retrieve sediment traps. There are other hazards like bad weather and high chances of accident during deployment, as was encountered by this study too.

Use of thorium derived flux in conjunction with sediment traps can give a more robust estimation of flux (Gustaffson et al., 1997). ^{234}Th-flux method requires much less shiptime, is less prone to failure and has a robust standardized procedure which makes the data consistent

(Waples et al., 2006; Maiti et al., 2012). Thorium derived POC flux estimation is completely independent from trap estimation, and can be used to cross check feasibility of the data (Buesseler, 1991). At the same time, ^{234}Th derived flux is averaged over a period of ~3 weeks (Buesseler et al., 1998; 2001), which is in sync with the biological particle dynamics in upper ocean. Averaging over a longer time scale also helps in ruling out POC flux caused by any temporary or local bloom, which can potentially upset sediment trap data.

4.2 ^{238}U-^{234}Th Analyses in Water Column

Uranium is a conservative element in sea water, which enables the estimation of ^{238}U activity in sea water by multiplying a constant with salinity (Ku et al., 1977). ^{238}U activity was estimated by multiplying 0.0704 dpm PSU^{-1} with salinity from respective depths measured by the on-board CTD of R/V Walton Smith (Chen et al., 1986; Owens et al., 2011). For determining ^{234}Th activity in water column between 0-750m, 4 liter water samples were used from different depths. Samples were transferred from Niskin bottles to acid washed 4 lit TEFLON bottles through acid cleaned silicon pipes. A ^{230}Th spike was added with weight calibrated pipette, immediately after collecting the samples in bottles. Then the samples were acidified to pH 2 (concentrated HCl), shaken thoroughly and left undisturbed to equilibrate. Acidification helps taking out organic molecules in the sample, which can retain thorium in sample solution. After >8 hours, pH was brought back to 8 by addition of NH_4OH. Thorium was co-precipitated with MnO_2 by addition of $KMnO_4$ and $MnCl_2$ into the bottles (Benitez-Nelson et al., 2000; Pike et al., 2005, Rutgers van der Loeff et al., 2006). The precipitate was allowed to form for another >8 hours and then was filtered using 25mm diameter 1μm QMA filters (Quartz Micro-fiber, Whatman International Ltd., England). For analysis of β-emission in RISØ analyzer (developed by the Center for Nuclear Technologies, Technical University of Denmark), the filters with the precipitate were dried and fixed on RISØ cups, below one layer of Mylar and two layers of regular aluminium foil. The samples were analyzed in RISØ counter for estimating beta emission from ^{234}Th via ^{234m}Pa (E_{max} = 2.19 MeV). Then, the samples were stored for 6 months and recounted, to estimate background emission from long lived radioisotopes (Maiti et al., 2012).

A number of factors might cause loss of thorium from the samples during analysis, viz, imperfect precipitation, breaking of filters, leakages and spills (Pike et al., 2005), which are potential sources of underestimation. Hence it is important to quantify the loss of thorium during analysis in order to estimate original ^{234}Th activity in the samples. The filters were used to estimate method-recovery of thorium, following "2-spike" method (Rodriguez y Baena et al.,

2006). After recounting in RISØ counter, filters were dismounted from RISØ cups, spiked with 1gm ^{228}Th standard and sonicated in 10% H_2O_2: 8M HNO_3 solution. The solutions were left overnight to equilibrate. Then the sample solutions were passed through HNO_3-conditioned AG 1-X8 anion exchange columns where thorium ions were retained. After passing the samples, the columns were washed with 9M HCl and the final elute, concentrated in ^{230}Th and ^{228}Th was collected in 50ml beakers. The samples were then evaporated and reconstituted to 4.5ml 0.1N HNO_3 and thorium was extracted using chelating organic compound Thenoyl-triflouroacetone (TTA) in benzene solution. Samples were transferred to glass centrifuge tubes, 0.5ml TTA solution was added and vigorously shaken with the sample solution for 15-20 minutes to ensure maximum extraction of thorium. The tube was then centrifuged to separate out TTA layer on top of acid layer. The thorium enriched TTA solution was then added drop-wise and evaporated on heated steel discs. The TTA extraction process was repeated 3 times. The discs were then counted in Canberra Alpha-analyst. Method-recovery was estimated from the ratio of ^{230}Th (4.688 MeV [76.3%]; 4.621 [23.4%] MeV) and ^{228}Th (5.423 MeV [72.7%]; 5.341 [26.7%] MeV) using the following equation—

$$^{234}Th_{yield} = [^{230}Th_{net} / ^{230}Th_{std}] * [^{228}Th_{std} / ^{228}Th_{net}] * 100 \qquad -[4.1]$$

Method recovery estimations from 2012 cruise samples ranges between 60-105% excluding outliers.

4.3 POC/^{234}Th Ratios in Suspended Particulate Samples

Size fractionated particulate samples were collected using large volume submersible pumps (McLane Research Laboratories, Inc., Falmouth, USA) from 100m, 150m, 250m and 350m. Battery operated pumps were deployed at each station twice, before the deployment and retrieval of sediment traps. The pumps were programmed to pump sea water for 4 hours, with a velocity 4-6 L min^{-1}, a total of ~600-950 L water was pumped. The pump-inlets were fitted with modified filter heads designed to keep out swimmers and prevent washing out of particles from the filters (Lam et al., 2007). Each filter head was fitted with a screen followed by a filter of 142mm diameter. Acid cleaned 51µm Nitex screen, and below that, muffled (450ºC, 8 hours) 1µm QMA (Quartz Micro-fiber, Whatman International Ltd., England) filter (Buesseler et al., 1995, 2006) was used. After retrieving the pumps, 25mm diameter punches were subsampled from the QMAs, dried at 60°C, and mounted onto RISØ cups under one layer of Mylar and two layers of regular aluminium foil for ^{234}Th analysis in RISØ counter. The particles collected on

Nitrex screen was rinsed with 1µm filtered sea water onto 25mm diameter 1.2µm silver membrane filters (STERLITECH Corp., USA). The silver filters were also analyzed following the method mentioned above for ^{234}Th analysis in RISØ counter (Moran et al., 2003; Buesseler et al., 2006).

The particulate samples were recounted in RISØ counter after a 6 months interval to estimate background radiation from long lived radioisotopes. After recount was complete, the filters were dismounted from RISØ cups and one 12mm punch was taken from both QMA (1-51µm) and silver filters (>51µm) to estimate organic carbon content in the size fractionated particles. The 12mm punches were exposed to concentrated HCl vapor for 24 hours by generating vacuum inside a closed glass vessel. Exposure to acid ensures elimination of any inorganic carbon present in the samples (Stewart et al., 2011; Pike and Moran, 1997). After fumigation, filters were dried at 60°C. Sample blanks were prepared using the same materials and method. The samples and the blank filters were wrapped inside silver capsules. Atropine ($C_{17}H_{23}NO_3$) was used as standard (Costech Analytical Technologies, Inc.). The samples, blanks and standards were run in Perkin Elmer Series II CHNS/O 2400 analyzer. Blanks and standards were run after every 10 samples in order to monitor stability of the instrument during analysis.

4.4 POC Flux Calculations

A simple, one-box mass balance model was followed to calculate ^{234}Th flux from ^{238}U-^{234}Th disequilibrium (Broecker et al., 1973, Matsumoto, 1975 and Tanaka et al., 1983). The POC/^{234}Th ratio was estimated from four depths. POC flux at each depth was estimated by multiplying ^{234}Th flux of the corresponding depth with POC/^{234}Th ratio from the same depth (Buessler et al., 1992).

In the mass balance box model, the scavenging is assumed to be constant inside the box. The general design (Figure 4.1) of ^{234}Th activity in the box model involves a balance between continuous production from ^{238}U (source-1), radioactive decay of ^{234}Th (sink-1), removal onto rapidly sinking particles (sink-2), and transport into the box by advection and diffusion (source-2).

The temporal change in total ^{234}Th is expressed by the following equation –

$$\delta A_{Th} / \delta t = \lambda A_U - \lambda A_{Th} - P \pm V \qquad \text{— [4.2]}$$

Where A_U and A_{Th} are the ^{238}U and the total ^{234}Th activities in water column [dpm m^{-3}], respectively, λ is the decay constant of ^{234}Th (λ = 0.02876 day^{-1}), P [dpm m^{-2} d^{-1}] is the net removal flux of ^{234}Th, and V is the sum of the advective and diffusive fluxes.

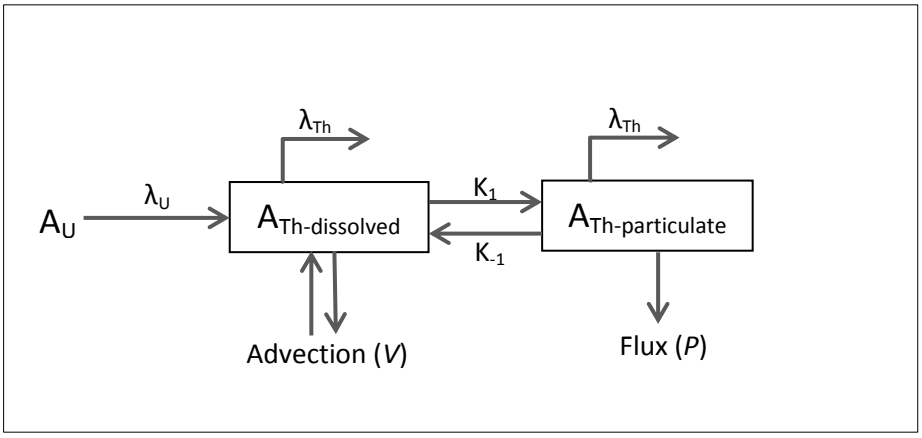

Figure 4.1. Box model of ^{234}Th activity in sea water (modified after Savoye et al., 2006). A_U is dissolved ^{238}U activity in sea water, $A_{Th\text{-}dissolved}$ is dissolved ^{234}Th activity in sea water, $A_{Th\text{-}particulate}$ is particulate ^{234}Th activity, λ_{Th} and λ_U are decay constants of ^{238}U and ^{234}Th respectively, and K_1 and K_{-1} are adsorption/desorption coefficients of ^{234}Th.

Steady state condition is assumed as repetitive sampling was not possible in the same locations (Buesseler et al., 2009). This implies that change of A_{Th} is assumed to be zero over time t, or, $[\delta A_{Th} / \delta t] = 0$. Physical advection and diffusion is also assumed to be negligible, or, $V = 0$. Hence equation [I] is reduced to —

$$0 = \lambda A_U - \lambda A_{Th} - P + 0$$

$$\text{or,} \quad P = \lambda A_U - \lambda A_{Th} \qquad \text{— [4.3]}$$

Then, equation [II] is integrated over depth z to obtain ^{234}Th-flux in the water column of height z —

$$Flux_{Th} = \lambda \int (A_U - A_{Th})\, dz \qquad \text{— [4.4]}$$

The ratio of [POC/ $A_{Th\text{-}particulate}$] is estimated from the size fractionated particulate samples. Particles of size 51μm or larger were used to calculate POC flux, as this size fraction constitutes the major portion of the sinking particle pool (Buesseler et al., 2006). The following

equation was used to calculate POC flux from particulate POC/^{234}Th ratio and water column ^{234}Th-flux —

$$Flux_{POC} = Flux_{Th} * (POC/ A_{Th})_{particulate} \quad \text{— [4.5]}$$

4.5 Results and Discussion

In this study, ^{234}Th-flux was estimated from ^{238}U-^{234}Th disequilibrium in water column (Table 4.1). Particulate POC/^{234}Th ratio was estimated from 4 depths – 100m, 150m, 250m, 350m. POC/^{234}Th ratio from a depth was multiplied with water column ^{234}Th-flux at the same depth, to estimate POC flux at that depth.

Table 4.1. Water column ^{234}Th-flux from 3 stations in 2012, compared with ^{234}Th-flux in sediment traps from 2 stations. Sediment trap ^{234}Th-flux is lower than water column ^{234}Th-flux. Change in flux over depth is negligible. Pattern of flux is similar between profiles (see Figure 4.2).

	Depth [m]	Water Column ^{234}Th-flux [dpm m^{-2} day^{-2}]		Trap derived ^{234}Th-flux [dpm m^{-2} day^{-2}]
NDWH	150	1886.99 ±1038.91	2605.56 ±946.95	–
	250	2185.31 ±2041.69	3392.36 ±1654.23	–
	350	1915.79 ±2165.79	3413.17 ±2452.95	–
DWH	150	1956.17 ±1132.12	2074.68 ±1696.42	966.00 ±531.49
	250	1999.69 ±2279.57	1906.65 ±3531.69	1317.47 ±287.83
	350	1824.59 ±3479.23	1360.34 ±5502.91	759.88 ±340.08
SDWH	150	1021.09 ±1295.10	1552.86 ±880.06	1071.54 ±255.86
	250	1242.69 ±2417.01	1754.80 ±1637.10	1067.17 ±341.23
	350	1152.96 ±3958.40	1544.95 ±2354.77	651.05 ±259.50

Water column ^{234}Th and ^{238}U activity profiles were used to estimate disequilibrium of ^{234}Th with respect to ^{238}U (see Figure 4.2). ^{238}U activity profiles are almost vertical, near-straight lines showing negligible or no change with depth. ^{234}Th activities are in equilibrium with ^{238}U at surface, decrease with depth, reach minima between 50-150m, and then again attain equilibrium with ^{238}U below 200m. ^{234}Th activities are found excess (than ^{238}U) between 250-350m depth, probably due to degradation of organic particles, which causes desorption of ^{234}Th into seawater. ^{234}Th-fluxes were calculated from the ^{238}U-^{234}Th disequilibrium (see discussion in Chapter 5.4). ^{234}Th-fluxes show a consistent trend in all three stations (Table 4.1, Figure 4.2). Change in fluxes is negligible between 150-250m in each profile. Water column ^{234}Th-fluxes were compared with

sediment trap derived ^{234}Th-fluxes from two stations (Table 4.1, Figure 4.2). Both methods yielded similar flux profiles. However, sediment trap derived ^{234}Th-flux was marginally lower than water column ^{234}Th-flux. Underestimation of flux from sediment traps is commonly observed in upper ocean and has been reported in multiple studies (Stewart et al., 2011; Hung et al., 2010).

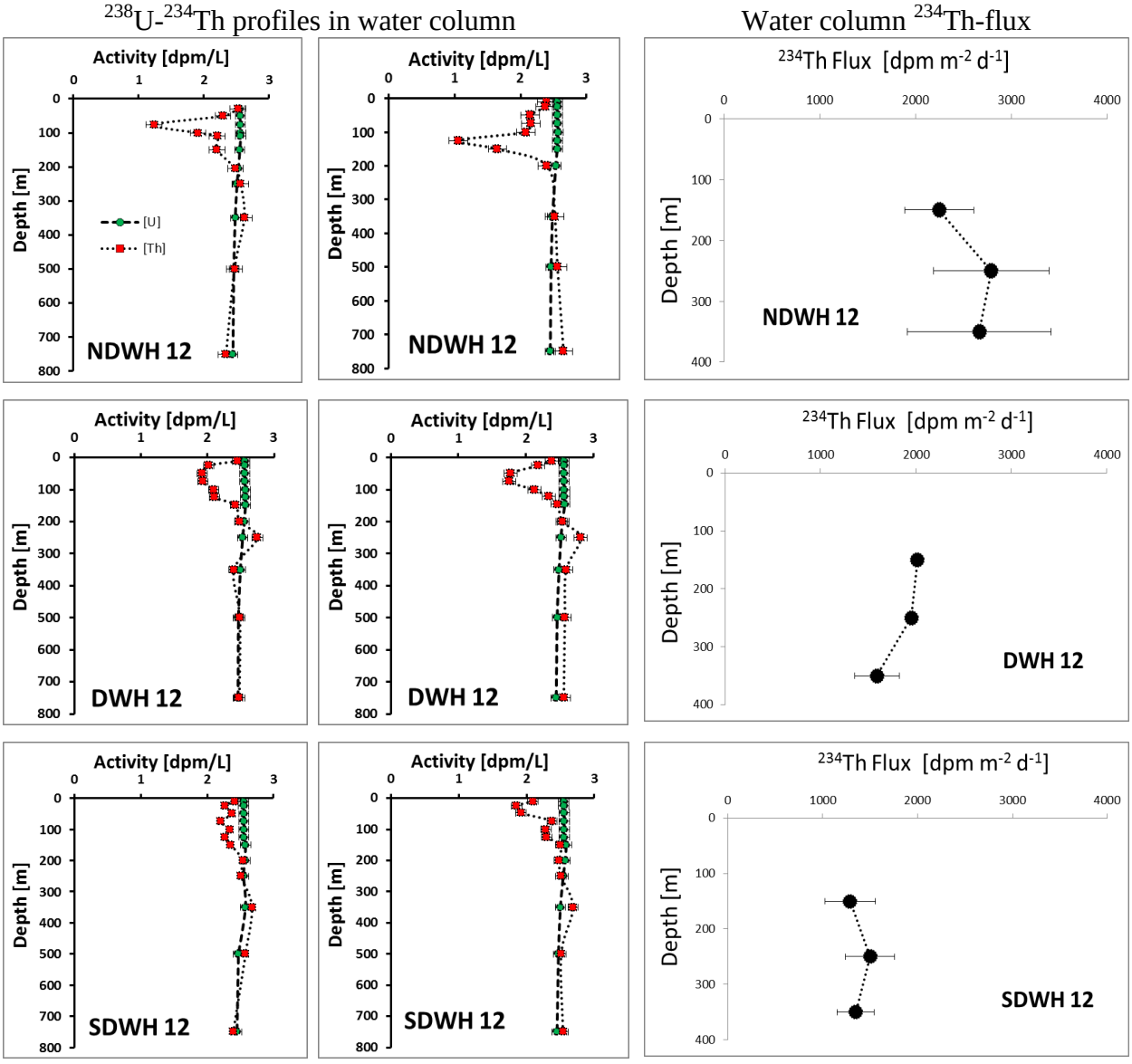

Figure 4.2. ^{238}U-^{234}Th profiles and ^{234}Th flux derived POC flux. ^{238}U activity profiles are almost vertical, near-straight lines showing negligible or no change with depth. ^{234}Th activity is in equilibrium with ^{238}U at surface, decreases with depth, reaches minima between 50-150m, regains equilibrium with ^{238}U below 200m, and becomes excess (than ^{238}U) between 250-350m depth. Change in ^{234}Th-flux is negligible over depth between 150-350m (see Table 4.1).

Size fractionated particulate POC/^{234}Th ratios were estimated in two size classes− 1-51 μm and >51 μm (see Figure 4.3). The ratio changes over depth, which is controlled by multiple factors. Thorium attaches to particle surface through sorption, whereas carbon content varies with the particle volume and composition (Santschi et al., 2006). Composition of particle-material can also control its "binding capacity" of thorium. As a result, particle volume/surface-area ratio and its composition, both play an important role in controlling the particulate

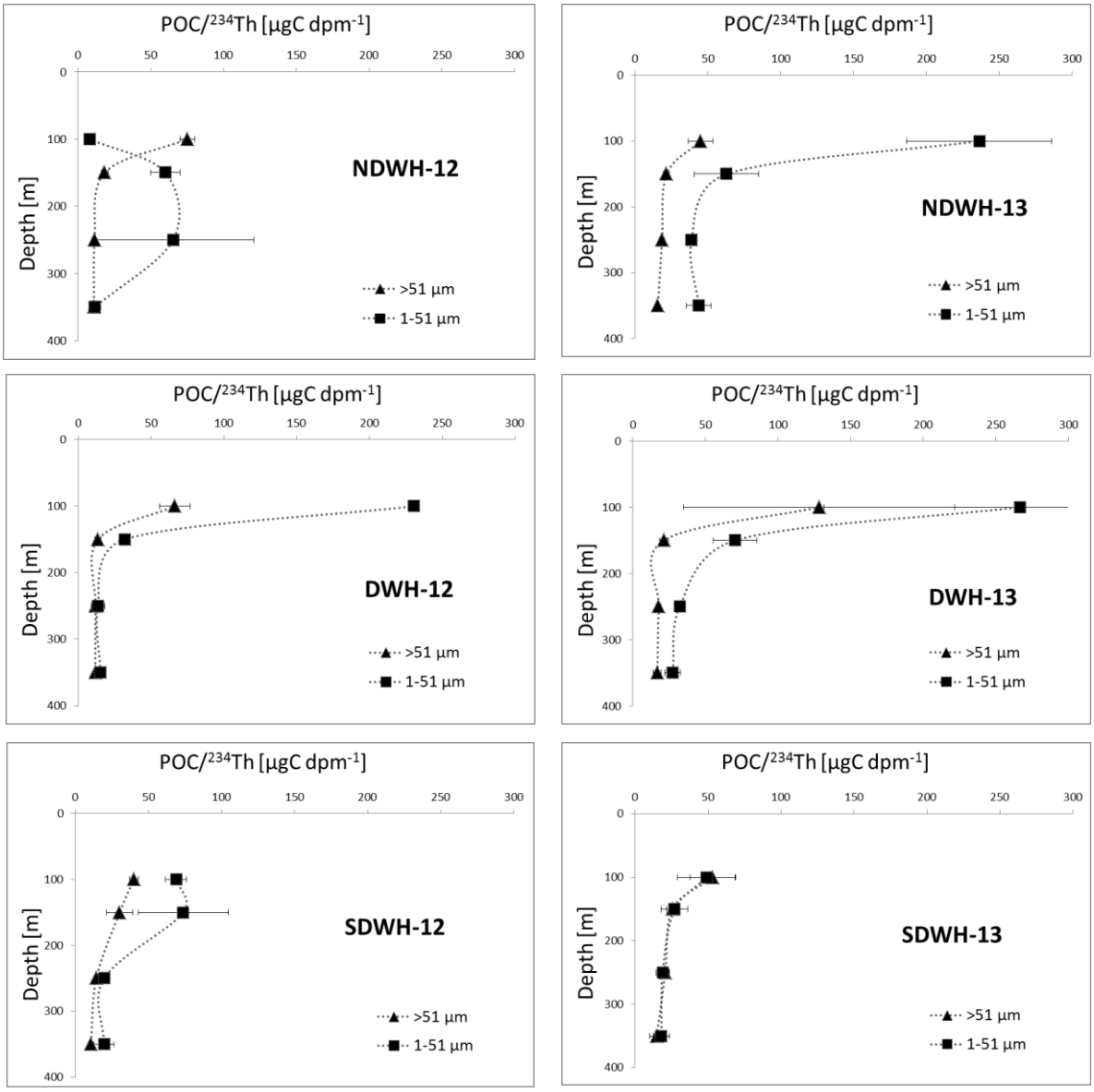

Figure 4.3. Size fractionated particulate POC/^{234}Th ratios. >51 μm particle size shows similar pattern of change over depth in 6 profiles. The ratio is high at 100m, decreases rapidly between 100-150m, and then decreases gradually between 150-350m (see Table 4.2). On the other hand, 1-51 μm particulate POC/^{234}Th profiles lack any consistent pattern.

POC/^{234}Th ratio (Buesseler et al., 2006). Biological activity, viz, degradation and assimilation in water column can also cause decrease of particulate carbon content (Buesseler et al., 2006). In this study, the particulate POC/^{234}Th ratio on 1-51 μm particles show a generally decreasing tend with depth. The depth profiles have maxima at 100m (48-267 μg dpm^{-1}), drops rapidly near 150m (26-71μg dpm^{-1}) and then decrease gradually with depth (Figure 4.3). On the other hand, >51 μm particulate POC/^{234}Th ratios are observed to have maxima at 100m (35-221 μg dpm^{-1}), drop rapidly near 150m (15-39 μg dpm^{-1}) and then decrease gradually with depth (see Figure 4.3, Table 4.2).

Table 4.2. POC/^{234}Th [μg dpm-1] ratio on >51um size fractionated particle. The ratio is similar in all 6 stations in 2012 and 2013. Their change over depth is also similar (see Figure 4.4).

	NDWH 12				NDWH 13			
Depth [m]	Pump 1		Pump 2		Pump 1		Pump 2	
100	79.94	±0.05%	69.85	±0.11%	53.25	±0.12%	36.31	±0.12%
150	20.52	±0.39%	15.93	±0.42%	23.66	±0.14%	19.35	±0.14%
250	10.51	±0.42%	12.01	±0.11%	16.53	±0.07%	20.29	±0.10%
350	10.39	±0.15%	11.21	±0.26%	14.94	±0.09%	16.21	±0.09%
	DWH 12				DWH 13			
	Pump 1		Pump 2		Pump 1		Pump 2	
100	55.94	±0.10%	76.89	±0.34%	221.57	±0.14%	35.06	±0.13%
150	15.52	±0.34%	11.61	±0.11%	18.55	±0.02%	24.47	±0.02%
250	11.88	±0.11%	11.95	±0.34%	19.55	±0.08%	16.32	±0.02%
350	10.68	±0.29%	12.72	±0.34%	14.26	±0.06%	19.72	±0.08%
	SDWH 12				SDWH 13			
	Pump 1		Pump 2		Pump 1		Pump 2	
100	42.90	±0.26%	37.31	±0.09%	37.75	±0.35%	68.57	±0.09%
150	39.17	±0.31%	21.51	±0.11%	29.42	±0.25%	21.53	±0.13%
250	14.16	±0.26%	14.65	±0.10%	23.49	±0.27%	17.64	±0.14%
350	11.37	±0.25%	9.97	±0.28%	19.77	±0.20%	9.66	±0.08%

POC flux was calculated by multiplying ^{234}Th flux with >51 μm particulate POC/^{234}Th ratio (Buesseler et al., 2006). POC flux, thus calculated, shows a consistent decrease with depth between 150m (41-33 mgCm^{-2}d^{-1}) to 350m (14-28 mgCm^{-2}d^{-1}) (Table 4.3) and has similar patterns in all the profiles (Figure 4.4). The decrease in POC flux is caused by remineralization of organic carbon in water column, which is also documented in the decrease of particulate POC/^{234}Th ratio. Remineralization causes loss of POC into soluble phase. As a result, ^{234}Th

relatively increase in particulate phase. Remineralization is quantified as the fraction of POC flux loss over a certain depth. Total remineralization between 150-350m water column was marginally higher in 2013 (43-65%) compared to the same in 2012 (31-42%) (Table 4.3).

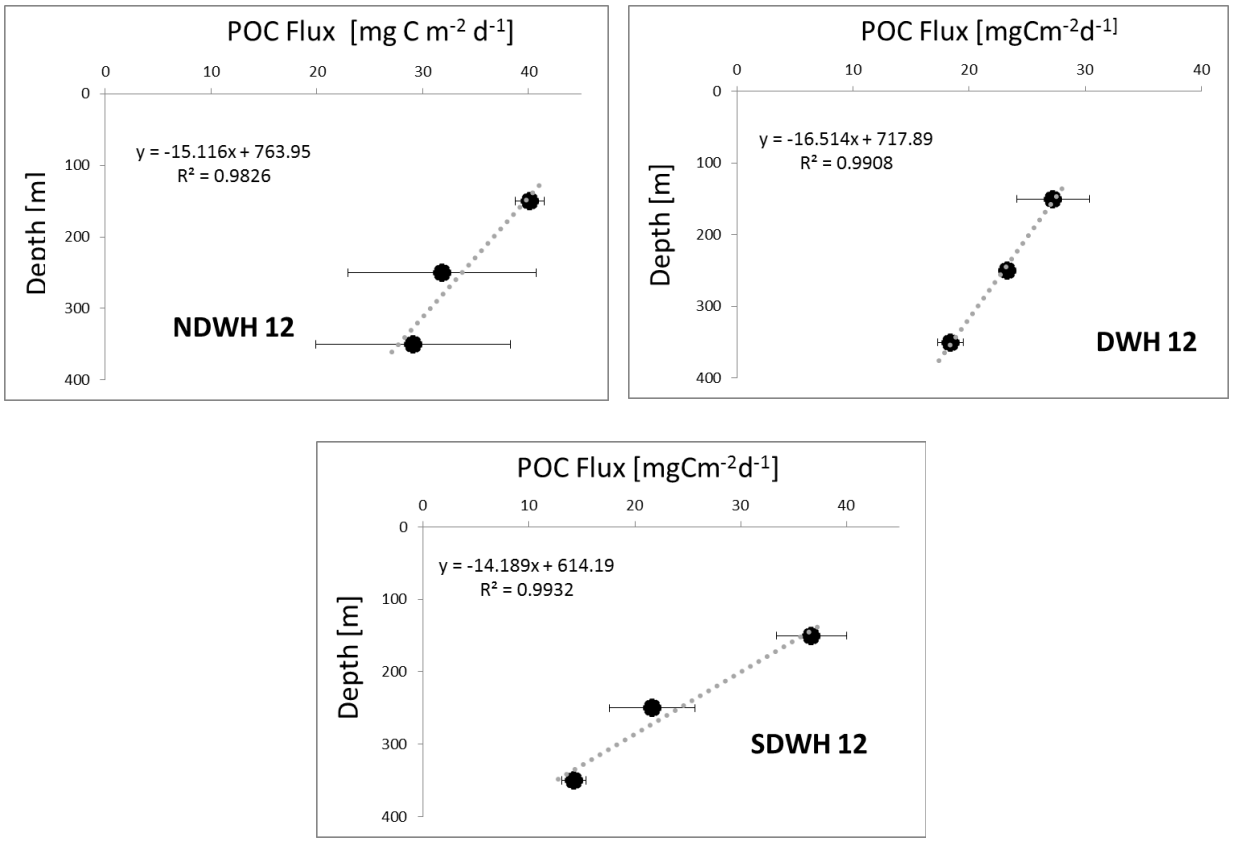

Figure 4.4. POC flux calculated from ^{234}Th flux. Change of POC flux with depth almost linear. Change of POC flux with depth less drastic in SDWH 12 compared to NDWH 12 and DWH 12.

Table 4.3. ^{234}Th-flux derived POC flux and remineralization between two flux depths. POC flux decreases with depth (see Figure 4.2).

	POC flux [mgC m^{-2} d^{-1}]		
	NDWH 12	DWH 12	SDWH 12
150m	40.11 ±1.39	27.23 ±3.13	36.70 ±3.30
Remineralization %	21	15	41
250m	31.85 ±8.89	23.27 ±0.49	21.65 ±4.06
Remineralization %	09	21	34
350m	29.08 ±9.18	18.40 ±1.09	14.26 ±1.15
Σ Remineralization %	27	32	61

^{234}Th derived POC flux data from our study was compared with sediment traps derived POC flux estimates (see Figure 4.5) and was also compared with another study from the Gulf of Mexico (Hung et al., 2010). Hung et al. collected samples only up to 140m, whereas our study was more focused towards the particle dynamics below the euphotic zone (150m-350m) to estimate remineralization and export efficiency (see discussion in Chapter 1 & 6). POC/^{234}Th ratio estimated by Hung et al. (2010) using 50-150µm particles at 140m was 1.6-6.7 µg dpm^{-1}, which does not match with the POC/^{234}Th ratio at 150m (11-39 µg dpm^{-1}) estimated from our study. The possible reason could be the different physical setting at their sampling locations. Hung et al. was more focused on understanding POC fluxes in ring or eddy systems in ocean, which can potentially influence POC/^{234}Th ratio.

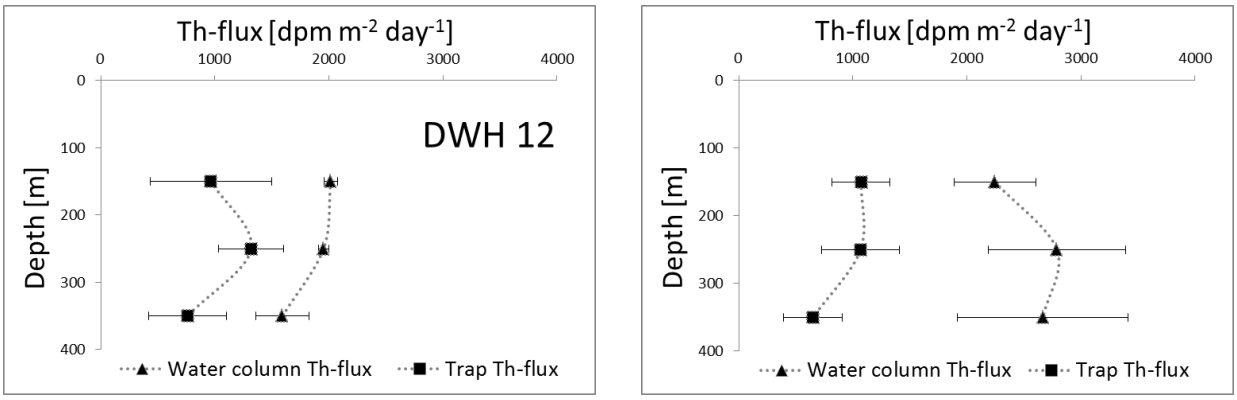

Figure 4.5. Comparison of water column and sediment trap derived ^{234}Th-flux. Change in flux over depth is negligible and trap derived flux is lower than water column ^{234}Th-flux.

Due to the dearth of available sediment trap data from the Gulf of Mexico, studies from other oligotrophic ocean were chosen to compare our data (see Table 4.4). Verdeny et al. (2009) formulated a universal method (also followed in this study) to calculate flux, and then recalculated POC flux from the published studies using their Po-flux and size fractionated particulate POC/^{210}Po ratio (Table 4.4), which were used to compare the results from this study. One of those studies from Bermuda Atlantic Time-series Study (BATS) site is an oligotrophic ocean with very low terrestrial influence, analogous to the Northern Gulf of Mexico. One of the BATS stations had low productivity (357.6 mg Cm^{-2}d^{-1}) and as a result remineralization was very low. The low remineralization is also reflected in the higher POC/^{234}Th at 300m (55.2 µg dpm^{-1}) than 150m (49.2 mg Cm^{-2}d^{-}1) in that particular station. The other two stations had

POC/^{234}Th comparable to our study (49-60 µg dpm^{-1} at 150m, 27-36 µg dpm^{-1} at 200m, 35-20 µg dpm^{-1} at 300m).

Table 4.4. Comparison of ^{234}Th derived POC fluxes with other studies from similar oceanographic settings. Flux values are in mgCm^{-2}day^{-1}.

Author	This study, 2012	Kim and Church, 2001.	Stewart et al., 2010.	Stewart et al., 2007.	Buesseler et al., 2008.	Maiti et al., 2008.
Location	Gulf of Mexico	Sargasso Sea	Bermuda, Atlantic	Mediterranean	Sargasso Sea	Tropical Pacific-Hawaii
150m	36-40	3.6-288	49-60		15.6-21.6	1.08-14.88
250m	21-31		27-36	48-216		
350m	14-29		35-20			

Chapter 5. ^{210}Pb-^{210}Po Derived POC Flux

5.1 Introduction

^{210}Pb-^{210}Po isotope pair can be used to estimate POC flux in the upper ocean following a principal similar to ^{238}U-^{234}Th. However, there are some key differences– ^{210}Po averages POC flux estimate over a period of approximately 6 months ($t_{1/2}$=138.3 days), and ^{210}Pb is not conservative in seawater, unlike ^{238}U. ^{234}Th adsorbs on to particle surfaces, whereas ^{210}Po is not only adsorbed on to particle surface but also bio-accumulated in organic matter. Depletion of ^{210}Po in the upper ocean water column was identified quite early (Cochran et al., 1983), but was not used to estimate particle flux until late 90's (Nozaki et al., 1997). Utilization of ^{210}Pb-^{210}Po disequilibrium in POC flux estimation is still limited (Verdeny et al., 2008), and its potential to estimate seasonal flux (~6 moths) is yet to be exploited extensively. However, quite a few studies in recent past have used this method along with other short lived isotopes and sediment trap based flux estimation, to compare seasonal flux variations (Stewart et al., 2011; Verdeny et al., 2008).

In open ocean, where terrestrial influences are minimal, the main source of ^{210}Pb in water column is from the in-situ decay of ^{226}Ra ($t_{1/2}$=1600 years) (Broecker et al., 1968; Ku and Lin, 1977). However, excess ^{210}Pb can also be introduced in the system from atmospheric flux. ^{222}Rn is formed in terrestrial soil, and is carried with airflow over the oceanic atmosphere. ^{210}Pb produced by decay of ^{222}Rn in atmosphere through multiple intermediate short-lived radionuclides, and has a short residence time of ~7 days in the atmosphere, before being deposited to surface-ocean (Moore et al., 1986; Turekian 1977). Due to the short residence time of ^{210}Pb in atmosphere, ^{210}Pb flux from atmosphere constitute only about 10–20% of the total ^{210}Pb in-put in ocean water. On the other hand, ^{210}Po is produced in ocean water column only by the in-situ decay of ^{210}Pb. ^{210}Pb decays to the intermediate short-lived radionuclide ^{210}Bi ($t_{1/2}$=5.01 days), which in turn decays to ^{210}Po.

^{210}Pb-^{210}Po should remain in secular equilibrium in a closed system, due to the short half-life of ^{210}Po ($t_{1/2}$=138.3 days) compared to its parent ^{210}Pb ($t_{1/2}$=22.2 years). However, ^{210}Po is often found depleted in upper ocean water column, due to scavenging by sinking particles (Bacon et al., 1976; Nozaki et al., 1976; Cochran, 1992). Polonium is more reactive to particles, compared to lead, which causes its more efficient scavenging compared to lead (Kharkar et al., 1976; Heyraud et al., 1976). Also, polonium is bio-accumulated into organic particles, while lead

only adsorbs to the surface of the particles. This property of ^{210}Pb-^{210}Po isotope pair enables its use as a proxy to organic materials fluxes (Stewart et al., 2007).

5.2 ^{210}Pb-^{210}Po Analyses in Water Column

For ^{210}Pb-^{210}Po analysis, a method similar to that described by Rigaud et al., 2013 was followed. 10 liter water samples were collected in a Niskin sampler, from 12 depths between 0-750m water column. Acid-cleaned 20 liter polypropylene cubitainers and silicon tubing was used to ensure minimal contamination while transferring the samples from Niskin. Right after collection, 100µl each of stable-Pb and ^{209}Po spike was added with calibrated pipettes as yield tracers of the two isotopes. Samples were acidified to pH 2 with concentrated HCl, shaken thoroughly and left undisturbed. Acidification helps in breaking down organic molecules, which can otherwise retain lead and polonium in the sample solution. After >8 hours, pH was brought back to 8 by the addition NH_4OH. Polonium and lead was co-precipitated with Fe^{3+}, by addition of $FeCl_3$ under controlled pH condition (Masque et al., 2002). The precipitate was allowed to settle for another 5-6 hours and then the effluent was decanted carefully from top to reduce sample volume to 1 liter. The samples were then transferred to 1l TEFLON coated bottles for a convenient transportation to lab.

In the lab, the precipitate was centrifuged to separate it completely from the effluent. The separated precipitate was then digested in an open vessel in 60ml concentrated HCl solution. After digestion, the solutions were evaporated and reconstituted to 70ml 1M HCl solution. At this stage, the solutions had yellowish tint due to the presence of Fe^{3+} ion. To eliminate Fe^{3+} from solution, chelating agent ascorbic acid was used (Friedrich, Rutgers van der Loeff, 2002). The beakers were set onto a hotplate with magnetic stirrer, TFLON stirrers were used and ascorbic acid was added slowly while stirring continuously, until the solutions became colorless. Next, the hotplate was set to 70°C temperature, with the stirrers spinning continuously. Silver-discs− one side polished, other side lacquered (diameter 3/4th inch), were dipped inside the beakers, mounted from TEFLON rods. Polonium ions were auto-deposited on the polished side of the silver discs. Auto-deposition was continued for 8 to 10 hours to achieve maximum deposition of polonium (Flynn, 1968; Rigaud et al., 2013). The silver discs were then counted in a Canberra Alpha Analyst to estimate ^{210}Po (5.0-5.2MeV) and ^{209}Po (4.8-5.0MeV).

^{210}Po is also produced inside the samples due to decay of ^{210}Pb, which is referred to as the "ingrowth of ^{210}Po". It is necessary to estimate the ingrowth of ^{210}Po from ^{210}Pb in the samples

during the time between collection to counting. ^{210}Po ingrowth estimation helps in calculating the ^{210}Pb-activity in the samples, and at the same time calculate ^{210}Po-activity at the time of collection. To estimate ^{210}Po-ingrowth, the "^{210}Po-clock" in the samples were "set to zero", or in other words− all ^{210}Po ions from the solutions was removed. This was done by column chemistry (Sarin et al., 1992). Sample solutions were passed through HCl-conditioned AG1-X8 anion exchange columns where polonium ions were retained and elute was collected in acid-cleaned 80ml beakers. The samples were stored in plastic bottles for 9 months to allow sufficient ^{210}Po ingrowth for analysis. After 9 months, 1ml aliquot was taken to analyze stable-Pb in ICP-OES to estimate method recovery of Pb isotopes (Rigaud et al., 2013). Pb recovery was found to range between ~50-75% with a few outliers. Then polonium auto-deposition was done on silver plates, following the same method described above, to estimate ^{210}Po ingrowth. The ^{210}Po ingrowth is caused by decay of ^{210}Pb present in the samples and was used to calculate ^{210}Pb activity in original sample.

5.3 POC/^{210}Po Ratios in Suspended Particulate Samples

Size fractionated particulate samples were collected using large volume submersible pumps (McLane Research Laboratories, Inc., Falmouth, USA) from 100m, 150m, 250m and 350m. Battery operated pumps were deployed at each station twice, before the deployment and retrieval of sediment traps. The pumps were programmed to pump sea water for 4 hours, with a velocity 4-6 L min^{-1}, a total of ~600-950 L water was pumped. The pump-inlets were fitted with modified filter heads designed to keep out swimmers and prevent washing out of particles from the filters (Lam et al., 2007). Each filter head was fitted with a screen followed by a filter of 142mm diameter. Acid cleaned 51µm Nitex screen, and below that, muffled (450ºC, 8 hours) 1µm QMA (Quartz Micro-fiber, Whatman International Ltd., England) filter (Buesseler et al., 1995, 2006) was used. After retrieving the pumps, 25mm diameter punches were subsampled from the QMAs. The particles collected on Nitrex screen was rinsed with 1µm filtered sea water onto 25mm diameter 1µm QMAs. All the QMA filters were dried at 60°C, and preserved in petri dishes for further analysis in lab.

In lab, the sample filters were spiked with ^{209}Po and stable-Pb yield tracers, and then microwave digested in closed vessel with aqua regia and 10% concentrated HF solution. After digestion, the sample solutions were evaporated and reconstituted to 70ml 1M HCl solution. Then polonium auto-deposition was performed on silver discs following the same method mentioned above and the discs were run in Canberra Alpha Analyst (Flynn, 1968; Fleer and

Bacon, 1984; Stewart et al., 2011). After auto-deposition, the samples were stored in plastic bottles for 9 months and then recounted again to estimate ^{210}Po in-growth from ^{210}Pb (Stewart et al., 2011). The ^{210}Po ingrowth estimation was used to calculate ^{210}Pb in the particulate samples.

Replicate filter samples were used for organic carbon analysis, because ^{210}Po-^{210}Pb analysis is destructive. 12mm punches were taken from QMAs. The 12mm punches were exposed to concentrated HCl vapor for 24 hours by generating vacuum inside a closed glass vessel. Exposure to acid ensures elimination of any inorganic carbon present in the samples (Stewart et al., 2011; Pike and Moran, 1997). After fumigation, filters were dried at 60°C. Sample blanks were prepared using the same materials and method. The samples and the blank filters were wrapped inside silver capsules. Atropine ($C_{17}H_{23}NO_3$) was used as standard (Costech Analytical Technologies, Inc.). The samples, blanks and standards were run in Perkin Elmer Series II CHNS/O 2400 analyzer. Blanks and standards were run after every 10 samples in order to monitor stability of the instrument during analysis.

5.4 POC Flux Calculation

The one-box model used to estimate flux from ^{238}U-^{234}Th disequilibrium cannot be used for ^{210}Pb-^{210}Po isotope pair, because unlike ^{238}U, ^{210}Pb is particle reactive and is not conservative in sea water. Hence a modified, two-box model was used to estimate ^{210}Po-flux (Verdeny et al., 2008). POC/^{210}Po ratio was estimated from four depths. POC flux at each depth was estimated by multiplying ^{210}Po-flux of the corresponding depth with POC/^{210}Po ratio from the same depth (Stewart et al., 2011).

In the mass balance box model, the scavenging is assumed to be constant inside the box. The general design (Figure 5.1) of ^{210}Pb and ^{210}Po activity in the box model involves a balance between continuous production from the parent radionuclides (source-1), radioactive decay (sink-1), removal onto rapidly sinking particles (sink-2), and transport into/out of the box by advection and diffusion (source-2/sink-3).

The temporal change in total ^{210}Po is expressed by the following equation –

$$\delta A_{Po} / \delta t = \lambda A_{Pb} - \lambda A_{Po} - P \pm V \qquad \text{— [Equation 5.1]}$$

Where A_{Pb} and A_{Po} are the ^{210}Pb and ^{210}Po activities in water column [dpm m^{-3}], respectively, λ is the decay constant of ^{210}Po (λ = 0.005008 day^{-1}), P [dpm m^{-2} d^{-1}] is the net removal flux of ^{210}Po, and V is the sum of the advective and diffusive fluxes.

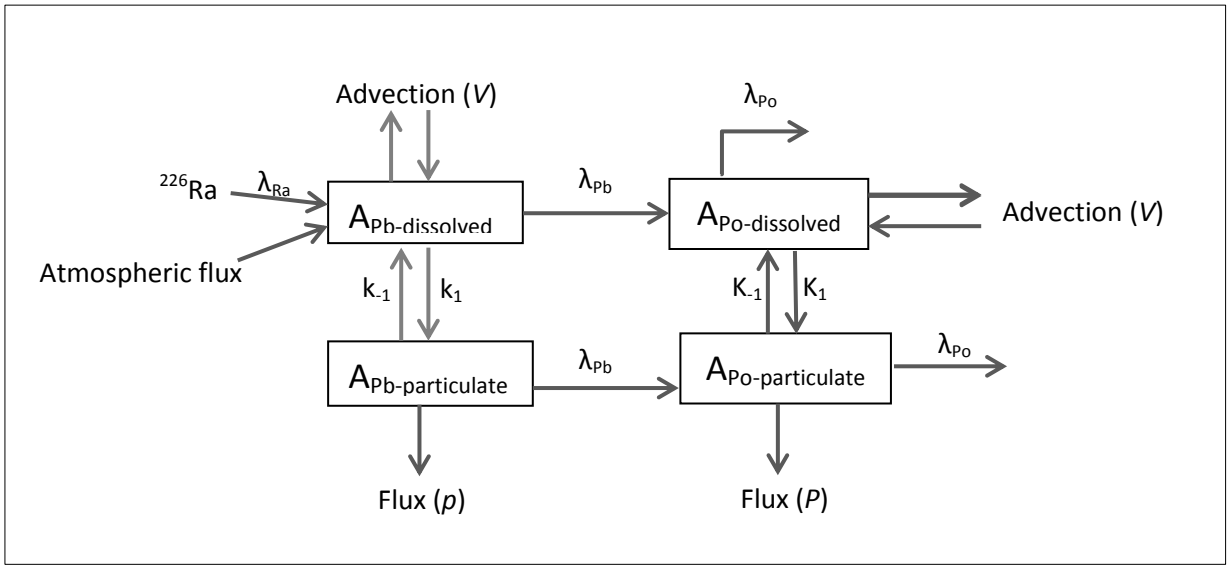

Figure 5.1. Box model of ^{210}Pb-^{210}Po activity in sea water. $A_{Pb\text{-}dissolved}$ and $A_{Po\text{-}dissolved}$ are dissolved activities in sea water, $A_{Pb\text{-}particulate}$ and $A_{Po\text{-}particulate}$ are particulate activities, $\lambda_{Ra,}$ λ_{Pb} and λ_{Po} are decay constants of ^{226}Ra, ^{210}Pb and ^{210}Po respectively. k_1, k_{-1} and K_1, K_{-1} are adsorption/desorption coefficients of ^{210}Pb and ^{210}Po Respectively (k<K). Flux (*p*) and Flux (*P*) is ^{210}Pb and ^{210}Po fluxes respectively.

Steady state condition is assumed as repetitive sampling was not possible in the same locations (Verdeny et al., 2008). This implies that change of A_{Po} is assumed to be zero over time *t*, or, $[\delta A_{Po} / \delta t] = 0$. Physical advection and diffusion is also assumed to be negligible, or, $V = 0$. Hence equation [4.1] is reduced to —

$$0 = \lambda A_{Pb} - \lambda A_{Po} - P + 0$$

$$\text{or,} \quad P = \lambda A_{Pb} - \lambda A_{Po} \qquad \text{— [5.2]}$$

Then, equation [4.2] is integrated over depth *z* to obtain ^{210}Po-flux in the water column of height *z* —

$$\text{Flux}_{Po} = \lambda \int (A_{Pb} - A_{Po})\, dz \qquad \text{— [5.3]}$$

The ratio of $[POC/A_{Po\text{-}particulate}]$ is estimated from the size fractionated particulate samples. Particles of size 51μm or larger were used to calculate POC flux, as this size fraction constitutes the major portion of the sinking particle pool (Stweart et al., 2011). The following equation was used to calculate POC flux from particulate POC/^{210}Po ratio and water column ^{210}Po-flux —

$$\text{Flux}_{POC} = \text{Flux}_{Po} * (POC/ A_{Po})_{\text{ particulate}} \qquad \text{— [5.4]}$$

5.5 Results and Discussion

In this study, ^{210}Po -flux was estimated from ^{210}Pb-^{210}Po disequilibrium in water column (Table 5.1). Particulate POC/^{210}Po ratio was estimated from 4 depths – 100m, 150m, 250m, 350m. POC/^{210}Po ratio from a depth was multiplied with water column ^{210}Po-flux at the same depth, to estimate POC flux at that depth.

Table 5.1. Water column 210Po-flux from 3 stations in 2012, compared with 210Po-flux in sediment traps from 2 stations. Sediment trap 210Po-flux is similar to water column 210Po-flux. Fluxes increase with depth. Pattern of change in fluxes is similar between profiles (see Figure 5.2 and 5.3).

	Depth [m]	Water Column ^{210}Po-flux [dpm m^{-2} day^{-1}]	Trap derived ^{210}Po-flux [dpm m^{-2} day^{-1}]
NDWH	150	42.58 ±1.67	—
	250	67.27 ±1.83	—
	350	82.69 ±1.90	—
DWH	150	58.72 ±1.67	68.41 ±3.42
	250	84.49 ±1.97	69.15 ±3.46
	350	96.45 ±2.08	78.91 ±3.95
SDWH	150	36.51 ±1.65	50.28 ±2.51
	250	53.58 ±1.86	72.13 ±3.61
	350	67.22 ±1.96	70.65 ±3.53

Water column ^{210}Pb and ^{210}Po activity profiles were used to estimate disequilibrium of ^{210}Po with respect to ^{210}Pb (see Figure 5.2). ^{210}Pb activity in water column varies between 4-16 dpm/100L. ^{210}Pb activities are high near surface, follow a zigzag pattern upto 200m and decrease steadily thereafter. Below 350m, ^{210}Pb and ^{210}Po profiles become parallel to each other. Similar ^{210}Pb activity profiles (ranging between 1.7-7.5 dpm/100L) from close locations in the Gulf of Mexico were reported by Baskaran et al. (2002). On the other hand, ^{210}Po activity is lower than ^{210}Pb in water column and varies between 3-10 dpm/100 L. The differences of ^{210}Pb and ^{210}Po activities are maximum near surface. ^{210}Po activity follows a generally vertical trend, with a pattern similar to that of ^{210}Pb, but with lower activities. ^{210}Po-fluxes were calculated from the ^{210}Pb-^{210}Po disequilibrium. ^{210}Po-fluxes show a consistent trend in all three stations, with an increase with depth between 150-350m in each profile (Table 5.1, Figure 5.2).

^{210}Pb-^{210}Po profiles | Water column ^{210}Po-flux

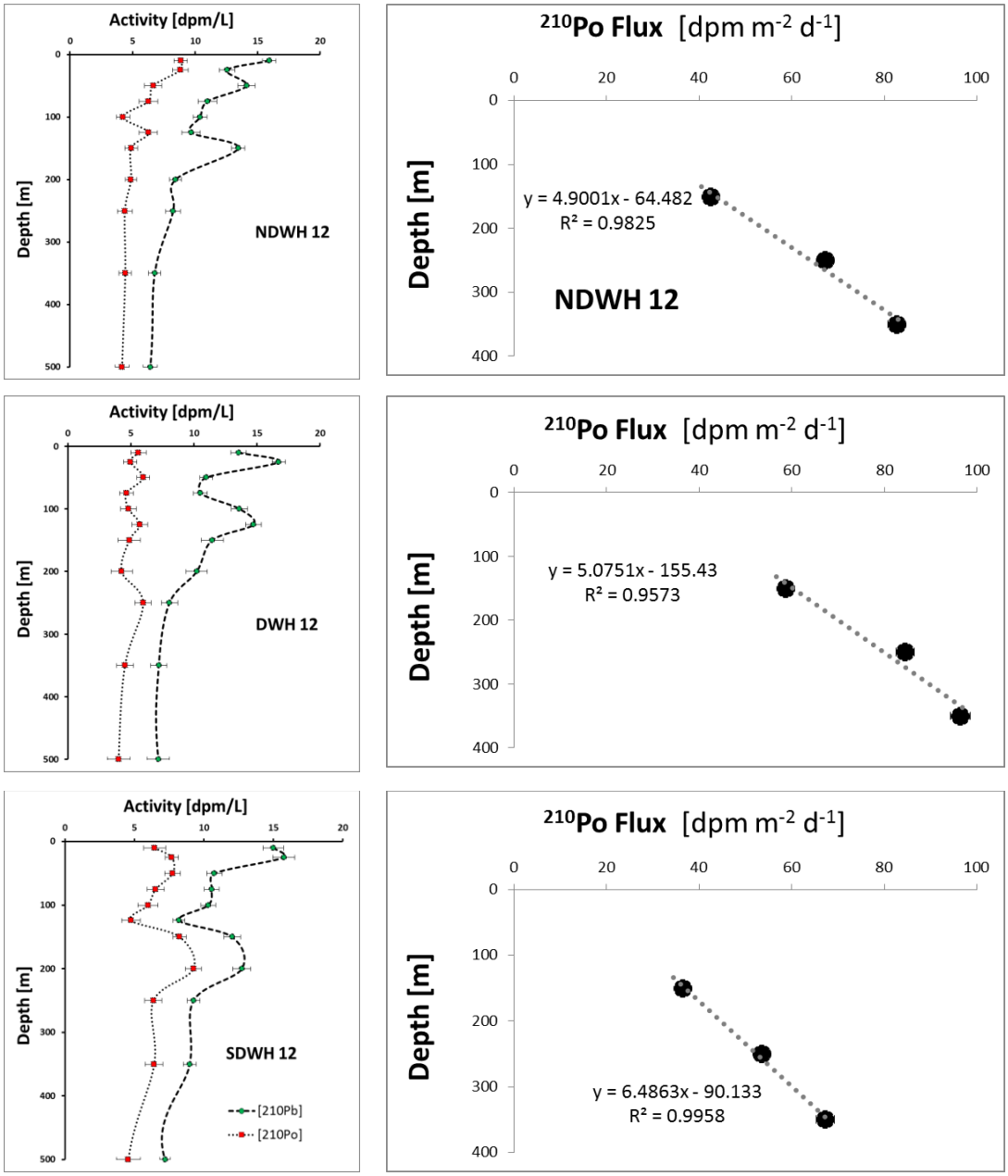

Figure 5.2. ^{210}Pb-^{210}Po profiles and ^{210}Po-flux. ^{210}Pb activities are high near surface, follow a zigzag pattern upto 200m and decrease steadily thereafter. Bellow 350m, ^{210}Pb and ^{210}Po profiles become parallel to each other. The differences of ^{210}Pb and ^{210}Po activities are maximum near surface. ^{210}Po activity follows a generally vertical trend, with a zigzag pattern similar to that of ^{210}Pb, with shallower kinks. ^{210}Po-fluxes show a consistent trend in all three stations− fluxes increase with depth between 150-350m in all profiles.

Water column ^{210}Po-fluxes were compared with sediment trap derived ^{210}Po-fluxes from two stations (Table 5.1, Figure 5.3). Both methods yielded very close flux values with a similar

trend of change with depth. Very close estimation of ^{210}Po flux from sediment traps and water column samples has also been reported in similar studies (Stewart et al., 2011).

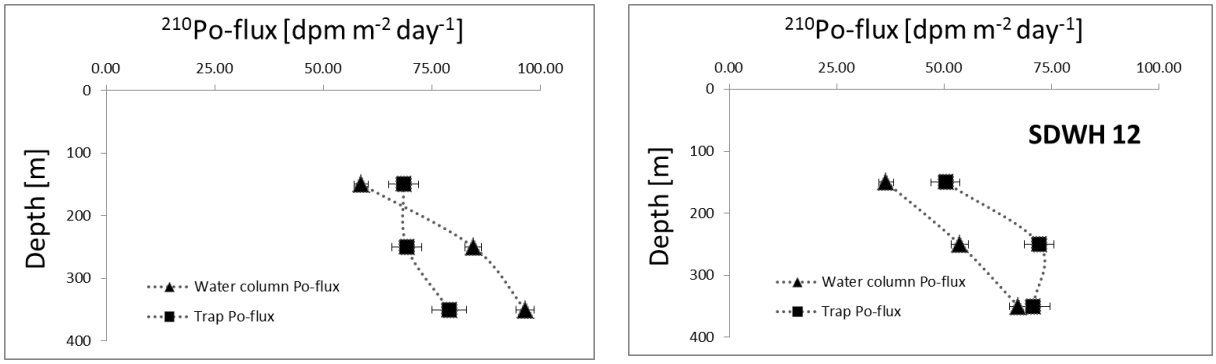

Figure 5.3. Comparison of water column and sediment trap derived ^{210}Po-flux. Flux profiles follow a generally common trend over depth. Fluxes derived from both the methods show similar flux values.

Size fractionated particulate POC/^{210}Po ratios were estimated from >51 μm particulate samples (see Table 5.2). The ratio shows a generally decreasing trend over depth. The decrease can be explained by remineralization of organic particles due to bacterial activity, which causes particulate polonium dissolution into sea water. The dissolution of ^{210}Po from particulate phase

Table 5.2. POC/^{210}Po [μg dpm^{-}1] ratio on >51um size fractionated particle. The ratio is similar in all 3 stations in 2012. The change over depth is also similar (see Figure 5.4).

Depth	NDWH	
[m]	Pump	Trap
150	507.12 ±25.36	—
250	192.90 ±9.65	—
350	117.80 ±5.89	—
	DWH	
	Pump	Trap
150	498.06 ±24.90	460.75 ±23.04
250	248.02 ±12.40	330.87 ±16.54
350	142.79 ±7.14	117.10 ±5.85
	SDWH	
	Pump	Trap
150	630.28 ±31.51	577.57 ±28.88
250	331.26 ±16.56	296.55 ±14.83
350	177.63 ±8.88	155.27 ±7.76

to water column is documented in ^{210}Po water column profiles, where ^{210}Po activity increases after ~250m. POC/^{210}Po ratio in >51 μm particles show similar pattern in all profiles. The ratio is maximum at 150m (507-630 μg dpm^{-1}), decreases to a large extent at 250m (192-332 μg dpm^{-1}) and then decreases gradually to 350m (see Figure 5.4, Table 5.2).

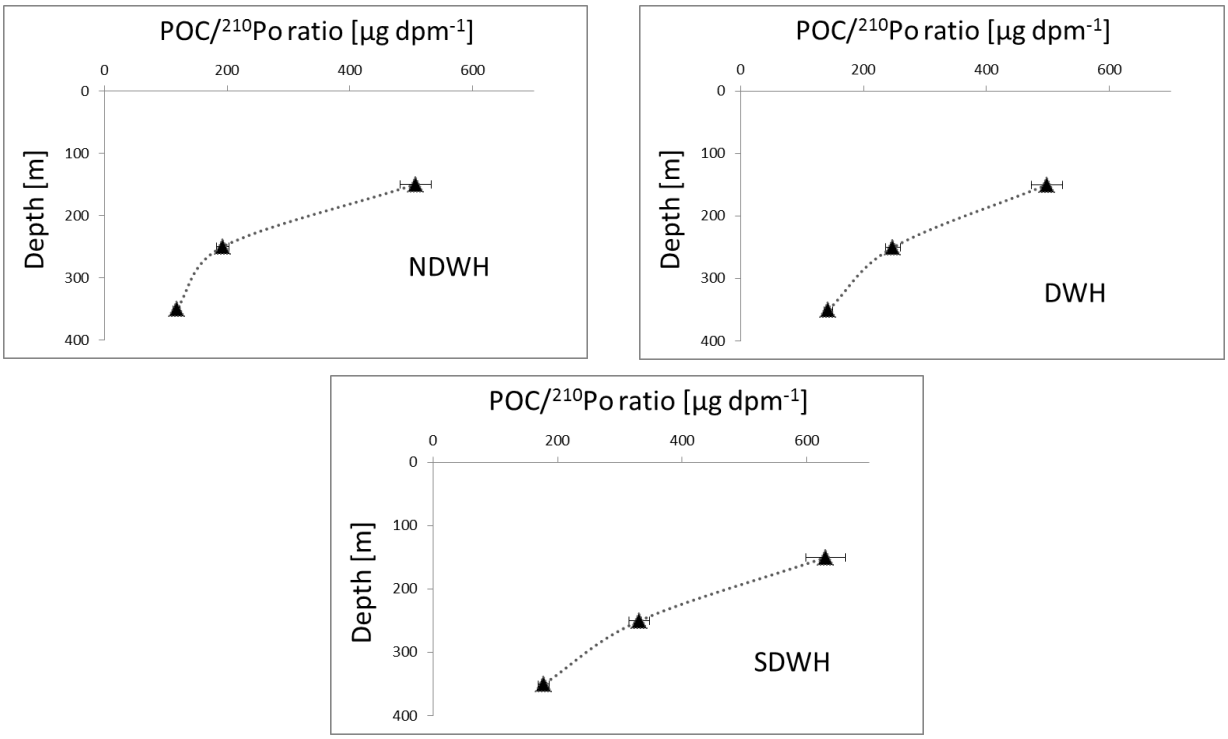

Figure 5.4. Size fractionated particulate POC/^{210}Po ratios. >51 μm particle size shows similar pattern of change over depth in all the 3 profiles. The ratio is high at 150m, decrease maximum between 150-250m, and then decrease between 150-350m, although comparatively less than the decrease between 150-250m (see Table 5.2).

POC flux was calculated by multiplying ^{210}Po-flux with >51 μm particulate POC/^{210}Th ratio on sinking particles (Verdeny et al., 2009). POC flux, thus calculated, has similar patterns in all the profiles (Figure 5.5) and shows a consistent decrease with depth between 150m (21-30 mgCm^{-2}d^{-1}) to 350m (9-14 mgCm^{-2}d^{-1}) (Table 5.3). The decrease in POC flux is caused by remineralization of organic carbon in water column, which is also documented in the decrease of particulate POC/^{210}Po ratio. Remineralization causes loss of POC into soluble phase. As a result, ^{210}Po relatively increase in particulate phase. Remineralization is quantified as the fraction of POC flux loss over a certain depth. Remineralization between 150-250m water column was higher (0.23-0.40) compared to the same in between 250-350m 0.25-0.34 (Table 5.3).

This study is the first initiative to estimate POC flux from ^{210}Pb-^{210}Po in the Gulf of Mexico. Hence, similar studies from other locations were used to compare with the results from this study (Stewart et al., 2010, 2011). Bermuda Atlantic Time-series Study (BATS) site is an oligotrophic ocean with very low terrestrial influence, similar to the open Gulf of Mexico. ^{210}Po derived POC flux profiles in this study showed a decreasing trend in flux over depth between 150-300m (150m— 24-50mgCm^{-2}day^{-1}; 300m— 6-18mgCm^{-2}day^{-1}) (Stewart et al., 2010, 2011).

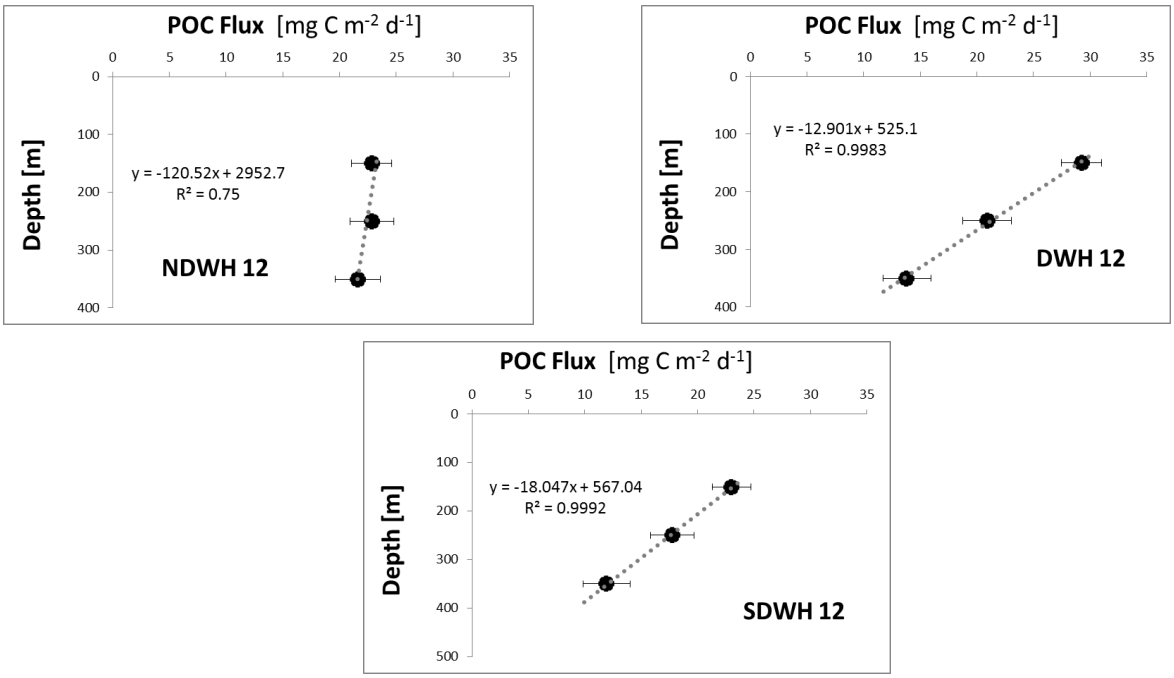

Figure 5.5. POC flux calculated from ^{210}Po-flux. Change of POC flux with depth highly linear. Change of POC flux with depth less drastic in NDWH 12 compared to NDWH 12 and DWH 12.

Table 5.3. ^{210}Th-flux derived POC flux and remineralization between two flux depths. POC flux decreases with depth (see Figure 5.3).

	POC flux [mgC m^{-2} day^{-1}]		
Depth [m]	NDWH	DWH	SDWH
150	21.60 ±1.75	29.25 ±1.75	23.01 ±1.74
Remineralization %	40	28	23
250	12.98 ±1.92	20.95 ±2.07	17.75 ±1.95
Remineralization %	25	34	33
350	9.74 ±1.99	13.77 ±2.18	11.94 ±2.06
Σ Remineralization %	55	53	48

^{210}Po derived POC flux estimates from around the globe were also used to compare with this study (Table 5.4). Verdeny et al. (2009) formulated a universal method (also followed in this study) to calculate flux, and then recalculated POC flux from the published studies using their Po-flux and size fractionated particulate POC/^{210}Po ratio (Table 5.4), which were used to compare the results from this study.

Table 5.4. Comparison of ^{210}Po derived POC flux with other studies from similar oceanographic settings. Flux values are in $mgCm^{-2}day^{-1}$.

Author	This study, 2012	Kim and Church, 2001.	Stewart et al., 2010.	Stewart et al., 2007.	Buesseler et al., 2008.	Maiti et al., 2008.
Location	Gulf of Mexico	Sargasso Sea	Bermuda, Atlantic	Mediterranean	Sargasso Sea	Tropical Pacific-Hawaii
150m	21-29	28-61	24-50		18-54	18-21
250m	12-20		33-85	14-31		
350m	9-14		6-18			

^{210}Po derived POC flux estimates from the Gulf of Mexico were found to be within range of flux estimates from other oligotrophic locations like the BATS (Stewart et al., 2010) and HOTS (Maiti et al., 2008).

Chapter 6. Conclusions

6.1 Introduction

The Northern Gulf of Mexico is one of the well-studied areas of global ocean, however there is only one reported estimate of upper ocean POC fluxes, and no reported estimate of upper ocean export efficiency of the "biological pump" from this region (Henson et al., 2012). The main objective of this study was to fill this gap our current knowledge, by estimating POC fluxes and export efficiencies in the upper ocean of Northern Gulf of Mexico. Understanding upper ocean POC fluxes is not only important because it set a limit to how much atmospheric carbon can be sequestered to the deeper ocean, but also ascertains how much carbon will be available to the benthic community which depends on rain of such organic matter as their major food source. In oligotrophic oceans like the Gulf of Mexico, POC is the main source of particles and is the key mechanism in removing particle reactive pollutants from the upper ocean water column. This study thus provides a better baseline data to estimate benthic organic carbon flux, allow us to better understand the possible impacts of future climate change on the biological pump in carbon sequestration on climate change.

In order to get a robust estimate of the POC fluxes in this region, we utilized three existing methods of POC flux measurement, which also provided a unique opportunity to intercompare the results from these three methods. These three methods are often used independently to estimate POC fluxes, however application of all the three methods in a single study site is rarely done, and till date only one such study is available (Stewart et al., 2011). Since each of these methods comes with their own set of assumptions and biases, it is important that these existing methods are compared under different oceanic settings as much as possible to understand their strength and limitation.

6.2 Seasonal Variability of POC Fluxes

The three methods used in this study averages POC fluxes over different time scales. Sediment trap directly estimates flux and the flux value is averaged over the time of deployment and gives the current estimation of flux averaged over 2-3 days. ^{234}Th and ^{210}Po provides indirect estimates of POC fluxes which averaged over timescales of ~1 month and ~6 months' time scale respectively (Buesseler et al., 2001; Verdeny et al., 2008).

The study region in open Gulf of Mexico experiences seasonal change in surface productivity which is generally high during the months of November to April and then decrease

during May to December (Biggs et al., 2008;). Thus by collecting samples in early April, we were able to quantify the average winter POC fluxes using ^{210}Po proxy. The seasonal average (21-30 mgCm^{-2}day^{-1}) were found to be similar to short term (^{234}Th, trap) POC fluxes (22-40 mgCm^{-2}day^{-1}), reflecting the oligotrophic and steady-state nature of the system (see Figure 6.1). The POC fluxes at DWH and SDWH sites were observed to be within the uncertainty range of each other for all the three methods, while POC fluxes derived from ^{210}Po were higher compared to ^{234}Th derived flux at the NDWH. The good agreement between the flux estimates carried out at stations DWH 12 and SDWH 12 using three different techniques, which integrates over very different timescales indicate that not only does all the three methods work well for our current setting but also, the seasonal variability of the POC fluxes at these two stations was limited. The disagreement between the calculated fluxes at NDWH could be due to passage of eddies or other mesoscale variability in the water column (Maiti et al., 2008).

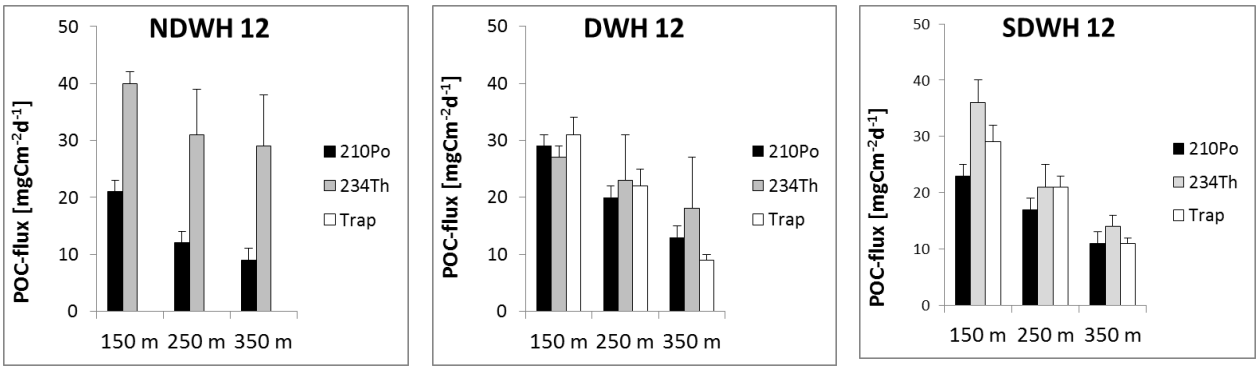

Figure 6.1. Temporal variability of POC flux. Black bar represents flux over last ~6 months (November-April), grey bar represents flux over last ~1 month (March-April), white bar represents current flux (mid-April).

The upper ocean POC fluxes estimated in this study were comparable to POC fluxes estimated by the only other available study carried out south west of this study area, in the Gulf of Mexico. POC fluxes estimated from that area ranges between 24-150 mgCm^{-2}day^{-1} (Hung et al., 2010).

6.3 Export Efficiency of the Biological Pump

Export efficiency is defined as the ratio of carbon utilized at surface ocean for photosynthesis, to the carbon sequestered from the upper ocean below the euphotic zone (Ducklow et al., 2001; Buesseler and Lampitt, 2008). This ratio, referred to as the efficiency of

the “biological pump”, provides an idea about what fraction of photosynthesized carbon is actually taken out from the atmosphere, and is potentially available for long term sequestration. In order to estimate the export efficiency, net primary production (NPP) data from the entire euphotic zone was collected from the sampling stations, on-board R/V Walton Smith (personal communication with Dr. Malinda Sutor, unpublished data). NPP were estimated at each sampling station, following a modified Winkler method. Winkler method is a gravimetric titration based method for determining dissolved oxygen in seawater (Helm et al., 2012). A comparison of export efficiency with NPP estimates also show an inverse relationship between the two (Figure 6.2 [left]). The export efficiencies were found to vary between 0.4–3% in this region which is similar to export efficiencies reported from HOTS and BATS (see Table 6.1).

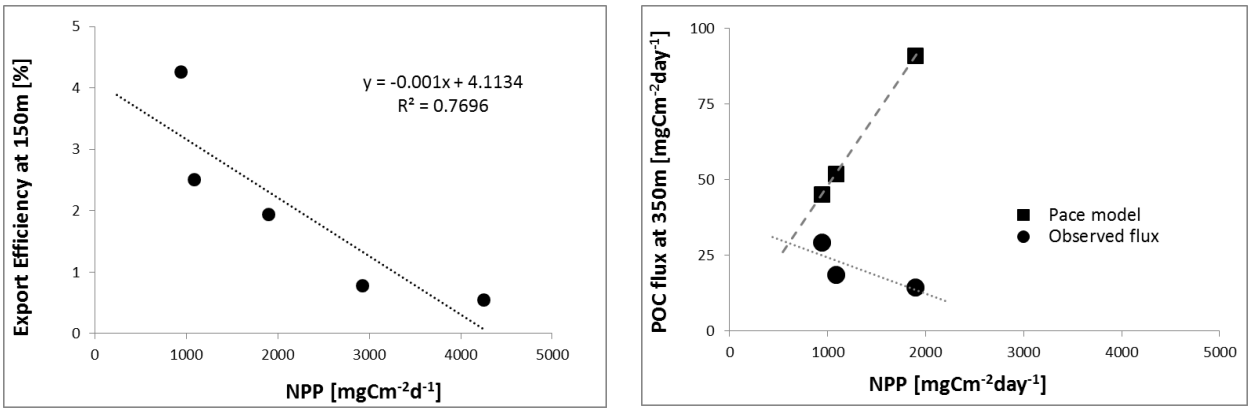

Figure 6.2. [Left] Plot of export efficiencies at 150m vs. Net Primary Production (NPP) in top 100m water column. Trend line shows an inverse linear (slope= -0.001, R^2=0.7) relation of export efficiency with NPP. [Right] Plot of POC fluxes at 350m from observed and Pace model derived data vs. NPP. Observed flux vs NPP plots have a negative sloping trend line, while model flux vs. NPP has a positive sloping trend line. The oppositely sloping trend lines clearly show their inverse relationship.

The inverse relation between primary productivity and export efficiency (Figure 6.2, [left]) implies that stations with higher NPP resulted in lower POC fluxes compared to the stations with lower NPP. This is contrary to the long held idea, that high NPP results in higher POC fluxes. However, recently published studies have also reported the inverse relationship from other locations (Maiti et al., 2008, 2013).The exact reason for such inverse relation need to be examined in conjunction with other plankton data which is beyond the review of this study. The inverse relationship found in our study questions the feasibility of POC flux estimations from sea surface productivity, which assumes a direct relationship between the two (Pace et al.,

1987). NPP vs. POC fluxes calculated using the Pace model, when plotted with NPP vs. observed POC fluxes indicate opposite trends (Figure 6.2 [right]), which further confirms the disagreement between the modeled and observed fluxes.

Table 6.1. Net primary production, POC fluxes and export efficiencies derived from 5 stations in 2012 and 2013.

	Net Primary Production [$mgCm^{-2}day^{-1}$]	POC flux [$mgCm^{-2}day^{-1}$]	Export efficiency [%]
NDWH 12			
100m	942.99		
150m		40.11	4.25
250m		31.85	3.38
350m		29.08	3.08
DHW 12			
100m	1085.58		
150m		27.23	2.51
250m		23.27	2.14
350m		18.40	1.69
SDWH 12			
100m	1898.93		
150m		36.70	1.93
250m		21.65	1.14
350m		14.26	0.75
DWH 13			
100m	4248.45		
150m		22.95	0.54
250m		13.95	0.33
350m		—	—
SDHW 13			
100m	2927.39		
150m		22.79	0.78
250m		14.25	0.49
350m		12.72	0.43

6.4 Comparison with Model POC Fluxes

Biggs et al. (2008) utilized a model proposed by Pace et al. (1987) to calculate POC fluxes from satellite derived chlorophyll/primary productivity data. Pace model (1987) uses a standardized equation ($POC\ flux = 3.523*depth^{-0.734}*NPP$) to calculate POC fluxes at specific depths from the surface NPP. However, several studies in the Gulf of Mexico show sediment

community oxygen consumption (SCOC) based carbon demands are 2-3 times more than the than the POC fluxes reaching the sea floor (Biggs et al., 2008, Rowe et al., 2008). This can be attributed to incorrect POC flux modelling, lateral input of carbon, or to other unknown processes (Rowe et al., 2008). It must be noted that Biggs et al., 2008 estimated surface production from satellite derived chlorophyll data which incorporated a wide range of error (~35%). In order to compare our observed data with Pace model, we utilized in-situ NPP data, measured at each station. The results indicate a 15-65% overestimation of POC fluxes by Pace model (1987) compared to the observed data in upper ocean (Figure 6.3).

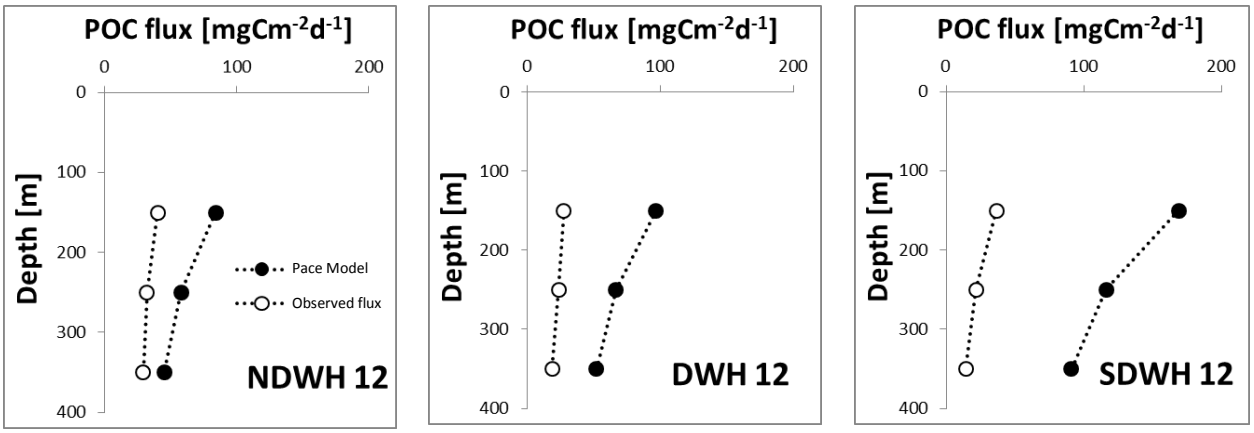

Figure 6.3. Comparison of POC flux estimated from NPP, using Pace model (1987) and POC flux estimated in field. Consistent overestimation can be seen in all three profiles with an overestimation of benthic flux ranging between 20-48%.

A discrepancy between modeled data and observed data of POC fluxes prompts refining of the available flux model, and as well designing area specific model for the Gulf of Mexico. It also highlights the fact that remote sensing based POC export estimates for this region utilizing Pace model (1987) should be treated with caution. However we must mention, although there is a big difference between Pace model (1987) and our in-situ POC flux estimates, the later was unable to close the discrepancy in benthic carbon-budget of this area (Rowe et al., 2008). The fact that observed POC flux estimates are lower than the modeled values implies that there exists an even bigger discrepancy in the benthic carbon budget than previous perceived, and the amount of carbon reaching the benthic community is probably lower than previously suggested estimates (Biggs et al., 2008).

References

Bacon, M. P., D. W. Spencer, and P. G. Brewer (1976), 210Pb/226Ra and 210Po/210Pb disequilibria in seawater and suspended particulate matter, *Earth and Planetary Science Letters*, *32*(2), 277-296, doi:http://dx.doi.org/10.1016/0012-821X(76)90068-6.

Benitez-Nelson, C. R., K. O. Buesseler, and G. Crossin (2000), Upper ocean carbon export, horizontal transport, and vertical eddy diffusivity in the southwestern Gulf of Maine, *Continental Shelf Research*, *20*(6), 707-736, doi:http://dx.doi.org/10.1016/S0278-4343(99)00093-X.

Benitez-Nelson, C. R., and W. S. Moore (2006), Future applications of 234Th in aquatic ecosystems, *Marine Chemistry*, *100*(3–4), 163-165, doi:http://dx.doi.org/10.1016/j.marchem.2005.10.010.

Biggs, D. C., C. Hu, and F. E. Müller-Karger (2008), Remotely sensed sea-surface chlorophyll and POC flux at Deep Gulf of Mexico Benthos sampling stations, *Deep Sea Research Part II: Topical Studies in Oceanography*, *55*(24–26), 2555-2562, doi:http://dx.doi.org/10.1016/j.dsr2.2008.07.013.

Broecker, W. S., J. Cromwell, and Y. H. Li (1968). Rates of vertical eddy diffusion near the ocean floor based on measurements of the distribution of excess 222Rn. *Earth and Planetary Science Letters, 5*(0), 101-105. doi: http://dx.doi.org/10.1016/S0012-821X(68)80022-6.

Bruland, K. W., K. H. Coale, and L. Mart (1985), Analysis of seawater for dissolved cadmium, copper and lead: An intercomparison of voltammetric and atomic absorption methods, *Marine Chemistry*, *17*(4), 285-300, doi:http://dx.doi.org/10.1016/0304-4203(85)90002-7.

Buesseler, K. O. (1991). Do upper-ocean sediment traps provide an accurate record of particle flux? *Nature*, 353, 420–423.

Buesseler, K. O., J. A. Andrews, M. C. Hartman, R. Belastock and F. Chai (1995). Regional estimates of the export flux of particulate organic carbon derived from thorium-234 during the JGOFS EqPac program. *Deep Sea Research Part II: Topical Studies in Oceanography*, *42*(2–3), 777-804. doi: http://dx.doi.org/10.1016/0967-0645(95)00043-P.

Buesseler, K. O., M. P. Bacon, J. Kirk Cochran, and H. D. Livingston (1992), Carbon and nitrogen export during the JGOFS North Atlantic Bloom experiment estimated from 234Th: 238U disequilibria, *Deep Sea Research Part A. Oceanographic Research Papers*, *39*(7–8), 1115-1137, doi:http://dx.doi.org/10.1016/0198-0149(92)90060-7.

Buesseler, K. O., L. Ball, J. Andrews, J. K. Cochran, D. J. Hirschberg, M. P. Bacon, M. Brzezinski (2001). Upper ocean export of particulate organic carbon and biogenic silica in the Southern Ocean along 170°W. *Deep Sea Research Part II: Topical Studies in Oceanography*, *48*(19–20), 4275-4297. doi: http://dx.doi.org/10.1016/S0967-0645(01)00089-3.

Buesseler, K. O., C. R. Benitez-Nelson, S. B. Moran, A. Burd, M. Charette, J. K. Cochran, T. Trull (2006). An assessment of particulate organic carbon to thorium-234 ratios in the ocean and

their impact on the application of 234Th as a POC flux proxy. *Marine Chemistry, 100*(3–4), 213-233. doi: http://dx.doi.org/10.1016/j.marchem.2005.10.013.

Buesseler, K. O., C. H. Lamborg, P. W. Boyd, P. J. Lam, T. W. Trull, R. R. Bidigare, J. K. B. Bishop, K. L. Casciotti, F. Dehairs, M. Elskens, M. Honda, D. M. Karl, D. Siegel, M. W. Silver, D. K. Steinberg, J. Valdes, B. Van Mooy and S. Wilson (2007). Revisiting Carbon Flux Through the Ocean's Twilight Zone. *Science*, 316: 567-570, DOI: 10.1126/science.1137959.

Buesseler, K. O., C. Lamborg, P. Cai, R. Escoube, R. Johnson, S. Pike, P. Masque, D. McGillicuddy, and E. Verdeny (2008), Particle fluxes associated with mesoscale eddies in the Sargasso Sea, *Deep Sea Research Part II: Topical Studies in Oceanography, 55*(10–13), 1426-1444, doi:http://dx.doi.org/10.1016/j.dsr2.2008.02.007.

Buesseler, K. O., and R. S. Lampitt (2008), Introduction to "Understanding the Ocean's biological pump: Results from VERTIGO", *Deep Sea Research Part II: Topical Studies in Oceanography, 55*(14–15), 1519-1521, doi:http://dx.doi.org/10.1016/j.dsr2.2008.04.009.

Buesseler, K. O., D. K. Steinberg, A. F. Michaels, R. J. Johnson, J. E. Andrews, J. R. Valdes, and J. F. Price (2000), A comparison of the quantity and composition of material caught in a neutrally buoyant versus surface-tethered sediment trap, *Deep Sea Research Part I: Oceanographic Research Papers, 47*(2), 277-294, doi:http://dx.doi.org/10.1016/S0967-0637(99)00056-4.

Chen, J. H., E. R. Lawrence, and G. J. Wasserburg (1986). 238U,234U and232Th in seawater. *Earth and Planetary Science Letters, 80*(3–4), 241-251. doi: http://dx.doi.org/10.1016/0012-821X(86)90108-1.

Cochran, J. K., M. P. Bacon, S. Krishnaswami, and K. K. Turekian (1983). 210Po and210Pb distributions in the central and eastern Indian Ocean. *Earth and Planetary Science Letters, 65*(2), 433-452. doi: http://dx.doi.org/10.1016/0012-821X(83)90180-2.

De La Rocha, C. L., and U. Passow (2007), Factors influencing the sinking of POC and the efficiency of the biological carbon pump, *Deep Sea Research Part II: Topical Studies in Oceanography, 54*(5–7), 639-658, doi:http://dx.doi.org/10.1016/j.dsr2.2007.01.004.

Dunne, John P., Jorge L. Sarmiento, and Anand Gnanadesikan (2007). A synthesis of global particle export from the surface ocean and cycling through the ocean interior and on the seafloor. *Global Biogeochemical Cycles*, 21, GB4006, doi:10.1029/2006GB002907.

Eppley, R.W., W.H. Berger, V. Smetacekm and G. Wefer (1989). New production: history, methods and problems. (Eds.), *Dahlem Workshop on "Productivity of the Ocean: Present and Past"*, Wiley, New York, pp. 85–97.

Fleer, A. P., and M. P. Bacon (1984). Determination of 210Pb and 210Po in seawater and marine particulate matter. *Nuclear Instruments and Methods in Physics Research, 223*(2–3), 243-249. doi: http://dx.doi.org/10.1016/0167-5087(84)90655-0.

Flynn, W. W. (1968). The determination of low levels of polonium-210 in environmental materials. *Analytica Chimica Acta, 43*(0), 221-227. doi: http://dx.doi.org/10.1016/S0003-2670(00)89210-7.

Friedrich, Jana, and M. M. Rutgers van der Loeff (2002). A two-tracer (210Po–234Th) approach to distinguish organic carbon and biogenic silica export flux in the Antarctic Circumpolar Current. *Deep Sea Research Part I: Oceanographic Research Papers, 49*(1), 101-120. doi: http://dx.doi.org/10.1016/S0967-0637(01)00045-0.

Gardner, W. D., J. B. Southard, and C. D. Hollister (1985), Sedimentation, resuspension and chemistry of particles in the northwest Atlantic, *Marine Geology*, *65*(3–4), 199-242, doi:http://dx.doi.org/10.1016/0025-3227(85)90057-X.

Gustafsson, Ö., P.M. Gschwend, K.O. Buesseler (1997). Settling removal rates of PCBs into the northwestern Atlantic derived from ^{238}U–^{234}Th disequilibria**.** Environmental Science and Technology, 31, pp. 3544–3550.

Helm, I., L. Jalukse, and I. Leito (2012). A highly accurate method for determination of dissolved oxygen: Gravimetric Winkler method. *Analytica Chimica Acta, 741*(0), 21-31. doi: http://dx.doi.org/10.1016/j.aca.2012.06.049.

Honjo, S., S. J. Manganini, R. A. Krishfield, and R. Francois (2008), Particulate organic carbon fluxes to the ocean interior and factors controlling the biological pump: A synthesis of global sediment trap programs since 1983, *Progress in Oceanography*, *76*(3), 217-285, doi:http://dx.doi.org/10.1016/j.pocean.2007.11.003.

Honjo, S. (1976). Coccoliths: Production, transportation and sedimentation. *Marine Micropaleontology*, *1*(0), 65-79. doi: http://dx.doi.org/10.1016/0377-8398(76)90005-0.

Hung, C.-C., C. Xu, P. H. Santschi, S.-J. Zhang, K. A. Schwehr, A. Quigg, L. Guo, G.-C. Gong, J. L. Pinckney, R. A. Long, and C.-L. Wei (2010), Comparative evaluation of sediment trap and 234Th-derived POC fluxes from the upper oligotrophic waters of the Gulf of Mexico and the subtropical northwestern Pacific Ocean, *Marine Chemistry*, *121*(1–4), 132-144, doi:http://dx.doi.org/10.1016/j.marchem.2010.03.011.

Ku, T.-L., K. G. Knauss, and G. G. Mathieu (1977), Uranium in open ocean: concentration and isotopic composition, *Deep Sea Research*, *24*(11), 1005-1017, doi:http://dx.doi.org/10.1016/0146-6291(77)90571-9.

Lamborg, C. H., K. O. Buesseler, J. Valdes, C. H. Bertrand, R. Bidigare, S. Manganini, S. Pike, D. Steinberg, T. Trull, and S. Wilson (2008), The flux of bio- and lithogenic material associated with sinking particles in the mesopelagic “twilight zone” of the northwest and North Central Pacific Ocean, *Deep Sea Research Part II: Topical Studies in Oceanography*, *55*(14–15), 1540-1563, doi:http://dx.doi.org/10.1016/j.dsr2.2008.04.011.

Lee, C., J.I. Hedges, S.G. Wakeham, N. Zhu (1992). Effectiveness of various treatments in retarding microbial activity in sediment trap material and their effects on the collection of swimmers. *Limnology and Oceanography*, 37 (1), pp. 117–130.

Longhurst, A. (1995), Seasonal cycles of pelagic production and consumption, *Progress in Oceanography*, *36*(2), 77-167, doi:http://dx.doi.org/10.1016/0079-6611(95)00015-1.

Maiti, K., K.O. Buesseler, S.M. Pike, C. Benitez-Nelson, P. Cai, W. Chen, K. Cochran, M. Dai, F. Dehairs, B. Gasser, R.P. Kelly, P. Masque, L.A. Miller, J.C. Miquel, S.B. Moran, P.J. Morris, F. Peine, F. Planchon, A.A. Renfro, M. Rutgers van der Loeff, P.H. Santschi, R. Turnewitsch, J.T. Waples, and C. Xu (2012). Intercalibration studies of short-lived thorium-234 in the water column and marine particles. *LandO Methods*, 10: 631-644.

Maiti, K., M.A. Charette, K.O. Buesseler and M. Kahru (2013). An inverse relationship between production and export in the Southern Ocean.*Geophysical Research Letters*, 40: 1-5, doi:10.1002/grl.50219.

Maiti, K., C. R. Benitez-Nelson, Y. Rii, and R. Bidigare (2008). The influence of a mature cyclonic eddy on particle export in the lee of Hawaii. *Deep Sea Research Part II: Topical Studies in Oceanography*, *55*(10–13), 1445-1460. doi: http://dx.doi.org/10.1016/j.dsr2.2008.02.008.

Masqué, P., J. A. Sanchez-Cabeza, J. M. Bruach, E. Palacios, and M. Canals (2002). Balance and residence times of 210Pb and 210Po in surface waters of the northwestern Mediterranean Sea. *Continental Shelf Research*, *22*(15), 2127-2146. doi: http://dx.doi.org/10.1016/S0278-4343(02)00074-2.

Moore, R. M., and J. N. Smith (1986). Disequilibria between226Ra, 210Pb and 210Po in the Arctic Ocean and the implications for chemical modification of the Pacific water inflow. *Earth and Planetary Science Letters*, *77*(3–4), 285-292. doi: http://dx.doi.org/10.1016/0012-821X(86)90140-8.

Morrison, J. M. and W. D. Nowlin, Jr. (1977). Repeated nutrient, oxygen and density sections through the Loop Current. Journal of Marine Research, 35, 105-128.

Murray, J.W., J.N. Downs, S. Strom, C.-L. Wei, H.W. Jannasch (1989). Nutrient assimilation, export production and ^{234}Th scavenging in the eastern equatorial Pacific**.** *Deep-Sea Research*, 36 (10), pp. 1471–1489.

Nozaki, Y., J. Thomson, and K. K. Turekian (1976). The distribution of 210Pb and 210Po in the surface waters of the Pacific Ocean. *Earth and Planetary Science Letters*, *32*(2), 304-312. doi: http://dx.doi.org/10.1016/0012-821X(76)90070-4.

Nozaki, Y., J. Zhang, and A. Takeda (1997). 2I0Pb and210Po in the equatorial Pacific and the Bering Sea: the effects of biological productivity and boundary scavenging. *Deep Sea Research Part II: Topical Studies in Oceanography*, *44*(9–10), 2203-2220. doi: http://dx.doi.org/10.1016/S0967-0645(97)00024-6.

Owens, S. A., K. O. Buesseler, and K. W. W. Sims (2011), Re-evaluating the 238U-salinity relationship in seawater: Implications for the 238U–234Th disequilibrium method, *Marine Chemistry*, *127*(1–4), 31-39, doi:http://dx.doi.org/10.1016/j.marchem.2011.07.005.

Pace, M., G. Kanuer, D. Karl, J. Martin (1987). Primary production, new production, and vertical flux in the eastern Pacific Ocean. *Nature*, 325, pp. 803–804.

Pike, S. M., K. O. Buesseler, J. Andrews and N. Savoye (2005). Quantification of 234Th recovery in small volume sea water samples by inductively coupled plasma mass spectrometry. *Journal of Radioanalytical and Nuclear Chemistry*, 263(2): 355-360.

Pike, S. M., and S. B. Moran (1997), Use of Poretics® 0.7 μm pore size glass fiber filters for determination of particulate organic carbon and nitrogen in seawater and freshwater, *Marine Chemistry*, *57*(3–4), 355-360, doi:http://dx.doi.org/10.1016/S0304-4203(97)00020-0.

Rigaud, S.**,** Puigcorbé, V., Camara-Mor, P., Casacuberta, N., Roca-Martí, M., Garcia-Orellana, J., Benitez-Nelson, C.R., Masque, P., Church, T., (2013). An assessment of the methods, calculation and uncertainties in the determination of 210Po and 210Pb activities in seawater. *Limnology and Oceanography Methodology: Methods*. 11, 561-571.

Rodriguez y Baena, A. M., J. C. Miquel, P. Masqué, P. P. Povinec, and J. La Rosa (2006), A single vs. double spike approach to improve the accuracy of 234Th measurements in small-volume seawater samples, *Marine Chemistry*, *100*(3–4), 269-281, doi:http://dx.doi.org/10.1016/j.marchem.2005.10.015.

S.A, O., B. K.O, L. C.H, V. J, L. M.W, J. R.J, S. D.K, and S. D.A (2013), A new time series of particle export from neutrally buoyant sediments traps at the Bermuda Atlantic Time-series Study site, *Deep Sea Research Part I: Oceanographic Research Papers*, *72*(0), 34-47, doi:http://dx.doi.org/10.1016/j.dsr.2012.10.011.

Santschi, P. H., J. W. Murray, M. Baskaran, C. R. Benitez-Nelson, L. D. Guo, C. C. Hung, Roy-Barman, M. (2006). Thorium speciation in seawater. *Marine Chemistry*, *100*(3–4), 250-268. doi: http://dx.doi.org/10.1016/j.marchem.2005.10.024.

Santschi, P. H., B. J. Presley, T. L. Wade, B. Garcia-Romero, and M. Baskaran (2001), Historical contamination of PAHs, PCBs, DDTs, and heavy metals in Mississippi River Delta, Galveston Bay and Tampa Bay sediment cores, *Marine Environmental Research*, *52*(1), 51-79, doi:http://dx.doi.org/10.1016/S0141-1136(00)00260-9.

Shannon, L. V., R. D. Cherry, and M. J. Orren (1970), Polonium-210 and lead-210 in the marine environment, *Geochimica et Cosmochimica Acta*, *34*(6), 701-711, doi:http://dx.doi.org/10.1016/0016-7037(70)90072-4.

Stewart, G., S. B. Moran, M. W. Lomas, and R. P. Kelly (2011), Direct comparison of 210Po, 234Th and POC particle-size distributions and export fluxes at the Bermuda Atlantic Time-series Study (BATS) site, *Journal of Environmental Radioactivity*, *102*(5), 479-489, doi:http://dx.doi.org/10.1016/j.jenvrad.2010.09.011.

Stewart, G., K. J. Cochran, J. Xue, C. Lee, S. T. Wakeham, R. A. Armstrong. J. Carlos Miquel (2007). Exploring the connection between 210Po and organic matter in the northwestern Mediterranean. *Deep Sea Research Part I: Oceanographic Research Papers*, *54*(3), 415-427. doi: http://dx.doi.org/10.1016/j.dsr.2006.12.006.

Stewart, G., S. Moran, L. Bradley, W. Michael, and R. P. Kelly (2011). Direct comparison of 210Po, 234Th and POC particle-size distributions and export fluxes at the Bermuda Atlantic Time-series Study (BATS) site. *Journal of Environmental Radioactivity*, *102*(5), 479-489. doi: http://dx.doi.org/10.1016/j.jenvrad.2010.09.011.

Turekian, Karl K. (1977). The fate of metals in the oceans. *Geochimica et Cosmochimica Acta, 41*(8), 1139-1144. doi: http://dx.doi.org/10.1016/0016-7037(77)90109-0.

van der Loeff, M. R., M. M. Sarin, M. Baskaran, C. Benitez-Nelson, K. O. Buesseler, M. Charette, M. Dai, Ö. Gustafsson, P. Masque, P. J. Morris, K. Orlandini, A. Rodriguez y Baena, N. Savoye, S. Schmidt, R. Turnewitsch, I. Vöge, and J. T. Waples (2006), A review of present techniques and methodological advances in analyzing 234Th in aquatic systems, *Marine Chemistry*, *100*(3–4), 190-212, doi:http://dx.doi.org/10.1016/j.marchem.2005.10.012.

Verdeny, E., P. Masqué, K. Maiti, J. Garcia-Orellana, J. M. Bruach, C. Mahaffey, and C. R. Benitez-Nelson (2008). Particle export within cyclonic Hawaiian lee eddies derived from 210Pb–210Po disequilibrium. *Deep Sea Research Part II: Topical Studies in Oceanography*, *55*(10–13), 1461-1472. doi: http://dx.doi.org/10.1016/j.dsr2.2008.02.009.

Waples, J. T., C. Benitez-Nelson, N. Savoye, M. Rutgers van der Loeff, M. Baskaran, and Ö. Gustafsson (2006), An introduction to the application and future use of 234Th in aquatic systems, *Marine Chemistry*, *100*(3–4), 166-189, doi:http://dx.doi.org/10.1016/j.marchem.2005.10.011.

Vita

Somiddho Bosu was born the son of Devamalya Bosu and Mahua Bosu in Kolkata, India, in the year 1987. He spent his youth in Kolkata and graduated from Hare School in 2006. He attended Presidency College (now Presidency University) and graduated with a Bachelor of Science in Geology in 2009. After his undergraduate studies, he moved out from Kolkata to attend the Indian Institute of Technology, Kharagpur for Master of Science in Geology. He graduated from Indian Institute of Technology, Kharagpur in 2011, and during his tenure at the institute, Somiddho was a member of the institute's swimming and water polo team and was awarded an honorable mention in the institute's yearbook in 2011. In 2012, he moved to United States of America and began graduate studies with Dr. Kanchan Maiti in the Department of Oceanography and Coastal Sciences at Louisiana State University. His master's research was focused in quantifying Particulate Organic Carbon Fluxes in the Northern Gulf of Mexico using radioisotope tracers. Somiddho defended his Master's thesis on May 5, 2014, with an aspiration for pursuing doctoral studies in future.